On the gravity-driven draining of a rivulet of a viscoplastic material down a slowly varying substrate

S. K. Wilson[1], B. R. Duffy and A. B. Ross

Department of Mathematics,
University of Strathclyde,
Livingstone Tower,
26 Richmond Street,
Glasgow G1 1XH,
United Kingdom

Running Title : Gravity-driven draining of a viscoplastic rivulet

10th January 2001, revised 14th June 2001

We use the lubrication approximation to investigate the steady locally unidirectional gravity-driven draining of a thin rivulet of viscoplastic material, modelled as a biviscosity fluid (or, as a special case, as a Bingham material), down a slowly varying substrate. In contrast to the earlier work on viscoplastic rivulets we consider small-scale flows, such as those found in many industrial coating and printing processes, in which surface-tension effects play a significant role. We interpret our results as describing a slowly varying rivulet draining in the azimuthal direction from the top to the bottom of a large horizontal circular cylinder. Provided that the yield stress is non-zero we find that the flow is always unyielded near the top of the cylinder (where the rivulet becomes infinitely wide in the transverse direction), and, except in the special case when the viscosity ratio is zero, near the bottom of the cylinder (where it becomes infinitely thick). For sufficiently small values of the prescribed volume flux the flow is unyielded everywhere, but for larger values of the flux the flow near the substrate in the centre of the rivulet is yielded. We obtain numerically calculated values of the semi-width of the rivulet and of the yielded region as well as of the maximum height of the rivulet and of the yielded region for a range of parameter values, and describe the asymptotic behaviour of the solution in the limits of large and small yield stress, large and small flux, and small viscosity ratio. In the special case of a Bingham material the flow near the top of the cylinder consists of an infinitely wide rigid and stationary plug, while elsewhere it consists of two rigid and stationary "levées" at the edges of the rivulet and a central region in which the flow near the free surface is a "pseudo-plug" whose velocity does not vary normally to the substrate, separated from the "fully plastic" flow near the substrate by a "pseudo-yield surface".

[1]Author for correspondence. Telephone : + 44 (0)141 548 3820, Fax : + 44 (0)141 552 8657, Email : s.k.wilson@strath.ac.uk

1 Introduction

The gravity-driven draining of a rivulet down an inclined substrate occurs in a number of practical situations ranging from many industrial devices and coating processes to a variety of geophysical flows. In practice many of the foodstuffs, paints and inks used in industrial coating and printing processes, as well as many of the muds and lavas found in geophysical contexts, are *viscoplastic*, that is to say they behave essentially like rigid solids when subjected to a small stress but flow more readily ("yield") when subjected to a large stress. The various constitutive equations that have been proposed to model viscoplastic materials are reviewed by Bird, Dai and Yarusso [1] and Barnes [2]. The existence of a *true* "yield stress" below which flow *never* occurs is the subject of a continuing rheological debate (see, for example, the review article by Barnes [2]). Notwithstanding this debate, the concept of a well-defined yield stress enshrined in the Bingham model and its generalisation the Herschel-Bulkley model (in both of which the material behaves like a perfectly rigid solid "plug" unless the stress exceeds the yield stress, but otherwise behaves like a viscous fluid) has proved a very useful idealisation in a wide range of practical applications. However, in other situations it is necessary to allow for some deformation at low shear rates. Several models have been proposed for these situations, including the biviscosity model employed in the present work. In practice the appropriate model to use will depend on the details of the specific flow under consideration.

However, as many authors have pointed out, a naive treatment of flows using either the Bingham or the Herschel-Bulkley model can give rise to the so-called "Bingham paradox", namely that regions of material that appear to be unyielded (and which are therefore supposed to behave like a rigid plug) are found to be deforming. In a pioneering paper Walton and Bittleston [4] undertook a careful asymptotic analysis of unidirectional axial flow of a Bingham material through a narrow eccentric annulus and found that the flow contains a "pseudo-

plug" region whose velocity is constant in the radial but *not* the azimuthal direction and in which the stress is just above the yield stress, as well as "fully plastic" regions in which the stress is significantly above the yield stress and a rigid "true-plug" region whose velocity is constant and in which the stress is below the yield stress. In an important recent paper Balmforth and Craster [3] showed that Walton and Bittleston's [4] work contains the essence of the resolution of the Bingham paradox. Balmforth and Craster [3] showed that, when interpreted correctly, the Bingham model does in fact lead to a consistent description of non-unidirectional two-dimensional thin-film flow, and that the apparently paradoxical solutions of earlier authors can be justified if they are interpreted correctly. In particular, Balmforth and Craster's [3] careful asymptotic analysis of non-unidirectional two-dimensional thin-film flow of a Herschel-Bulkley material down an inclined plane reveals that the "unyielded region" is in fact a pseudo-plug region in which the stress is just above the yield stress and that the "yield surface" is in fact a "pseudo-yield surface" separating the pseudo-plug and fully plastic regions. Wilson [5] independently obtained the corresponding results using the biviscosity model in the distinguished limit in which the aspect ratio of the flow and the ratio of the two characteristic viscosities in the model approach zero together. In particular, he found that in this limit the true yield surface divides the pseudo-plug region into regions in which the stress is either significantly below or just above the yield stress. Balmforth and Craster's [3] results for a Bingham material are recovered as a special case of Wilson's [5] analysis. Recently Ross, Wilson and Duffy [6] used the same biviscosity model to study two-dimensional thin-film flow round a large horizontal stationary or rotating cylinder. In the present work we shall allow for the possibility of some deformation at low stresses by employing the biviscosity model. Note that the Bingham model (in which such deformation is impossible) can be recovered as a special case of the biviscosity model.

The pioneering analysis of the steady unidirectional flow of a uniform rivulet of Newtonian

fluid down an inclined plane in the presence of significant surface-tension effects was undertaken by Towell and Rothfeld [7]. This work was subsequently extended by Rosenblat [8] to study flow of a viscoelastic fluid and by Alekseenko, Geshev and Kuibin [9] to study flow down the lower surface of an inclined circular cylinder. Duffy and Moffatt [10] used the lubrication approximation employed by Allen and Biggin [11] to obtain analytically the leading-order solution for Newtonian rivulet flow down a planar substrate in the special case when the cross-sectional profile of the rivulet in the direction transverse to the flow is thin. Duffy and Moffatt [10] calculated the shape of the rivulet (and, in particular, its width and maximum height) as a function of α, the angle of inclination of the substrate to the horizontal, for $0 \leq \alpha \leq \pi$. Duffy and Moffatt [10] also interpreted their results as describing the locally unidirectional flow down a locally planar substrate whose local slope α varies slowly in the flow-wise direction and, in particular, used them to describe the flow in the azimuthal direction round a large horizontal circular cylinder. Wilson and Duffy [12] extended this analysis to study flow of a non-uniform rivulet down a slowly varying substrate with variation transverse to the direction of flow. Recently Holland, Duffy and Wilson [13] used the same approach to study flow of a non-uniform rivulet whose surface tension depends linearly on temperature down a slowly varying substrate that is uniformly hotter or colder than the surrounding atmosphere. Taking a somewhat different approach Smith [14] and Duffy and Moffatt [15] obtained similarity solutions of the thin-film equations describing the steady draining of a slender non-uniform rivulet of Newtonian fluid from a point source on an inclined plane in the cases of weak and strong surface-tension effects respectively. Both of these similarity solutions predict a varying contact angle at the contact line; recently Wilson, Duffy and Davis [16] showed how they can be modified to accommodate a fixed-contact-angle condition if sufficiently strong slip at the solid/fluid interface is incorporated into the model. Wilson and Burgess [19] generalised Smith's [14] similarity solution to flow of a power-law fluid.

There has been much less work on rivulets of viscoplastic material, and the work that has been undertaken is concerned exclusively with large-scale geophysical flows (such as flows of lavas and muds) in which surface-tension effects are insignificant. The pioneering analysis of the steady unidirectional flow of a uniform rivulet of Bingham material down an inclined plane in the absence of surface-tension effects was performed by Hulme [17]. His analysis predicts that the central portion of the rivulet is bounded laterally by stationary regions of unyielded material (which resemble the "levées" often observed in nature) that occur when the local height of the free surface falls below the "yield height" $\tau_y/\rho g \sin\alpha$, where τ_y and ρ denote the constant yield stress and density of the material, α the angle of inclination of the plane to the horizontal and g acceleration due to gravity. Unfortunately, as Coussot and Proust [18] pointed out, Hulme's [17] lateral force balance is erroneous, and the correct solution to the problem he posed has a uniform free surface in the central region of the rivulet whose height is everywhere equal to the yield height and so the rivulet is unyielded everywhere and hence stationary. Appreciating the shortcomings of the unidirectional-flow solution Coussot and Proust [18] derived the thin-film equation for a slender non-uniform rivulet of a Herschel-Bulkley material. This equation does not admit a similarity solution, but Coussot and Proust [18] did obtain a similarity solution to an approximate version of their equation which is in qualitative (but not quantitative) agreement with a series of their own experimental measurements made using various muds. Subsequently Wilson and Burgess [19] found that for the two experiments for which Coussot and Proust's [18] equation is appropriate, quantitative agreement can be obtained between the experimental measurements and numerically calculated solutions of the unapproximated equation.

As far as the authors are aware there has been no previous work on the problem addressed in the present paper, namely small-scale rivulet flow of viscoplastic materials, such as those found in many industrial coating and printing processes, in which surface-tension effects play a

significant role. Specifically in the present paper we shall follow the approach of Duffy and Moffatt [10] and use the lubrication approximation to investigate the steady locally unidirectional gravity-driven draining of a thin rivulet of viscoplastic material, modelled as a biviscosity fluid (or, as a special case, as a Bingham material), down a slowly varying substrate.

2 A Biviscosity Fluid

The governing equations representing conservation of mass and balance of momentum for steady flow of an incompressible fluid with constant density ρ take the form

$$\nabla \cdot \mathbf{u} = 0, \quad \rho(\mathbf{u} \cdot \nabla)\mathbf{u} = \nabla \cdot \boldsymbol{\sigma} + \rho \mathbf{g}, \tag{1}$$

where $\mathbf{u}$, $\boldsymbol{\sigma}$ and $\mathbf{g}$ denote the fluid velocity, stress tensor and acceleration due to gravity, respectively. In the present work we shall consider a biviscosity fluid whose constitutive law is given by

$$\boldsymbol{\sigma} = -p\mathbf{I} + \boldsymbol{\sigma}', \quad \text{where} \quad \boldsymbol{\sigma}' = \begin{cases} 2\mu_1 \mathbf{e}, & \tau \leq \tau_{\mathrm{y}}, \\ 2\left(\mu_2 + \dfrac{\tau_0}{q}\right)\mathbf{e}, & \tau > \tau_{\mathrm{y}}, \end{cases} \tag{2}$$

in which p is the pressure, $\mathbf{I}$ is the identity tensor, $\mathbf{e}$ is the rate-of-deformation tensor, q is the local shear rate and τ is a scalar measure of the local stress, given by

$$\mathbf{e} = \frac{1}{2}\left[(\nabla \mathbf{u}) + (\nabla \mathbf{u})^T\right], \quad q = \left[2\ \mathrm{tr}(\mathbf{e}^2)\right]^{1/2}, \quad \tau = \left[\frac{1}{2}\ \mathrm{tr}(\boldsymbol{\sigma}'^2)\right]^{1/2}. \tag{3}$$

The other four quantities in (2), namely the viscosities μ_1 and μ_2 and the stresses τ_0 and τ_{y}, are constant material parameters related by $\tau_{\mathrm{y}} = \mu_1 q_{\mathrm{y}} = \mu_2 q_{\mathrm{y}} + \tau_0$, where q_{y} is the value of the shear rate at which the "yield stress" τ_{y} is attained [20]. The relation between τ and q is given by $\tau = \mu_1 q$ when $q \leq q_{\mathrm{y}}$ and $\tau = \mu_2 q + \tau_0$ when $q > q_{\mathrm{y}}$, and is shown in Fig. 1. We note that $\tau_0 = \tau_{\mathrm{y}}(1 - \lambda)$, where the viscosity ratio λ is defined by $\lambda = \mu_2/\mu_1$. For $\tau \leq \tau_{\mathrm{y}}$ the fluid is "unyielded" and behaves like a Newtonian fluid with a "high" (constant) viscosity μ_1, while for $\tau > \tau_{\mathrm{y}}$ the fluid is "yielded" and behaves like a viscous fluid with a "low" (shear-rate-dependent) viscosity $\mu_2 + \tau_0/q$. In the present viscoplastic context $\mu_2 \leq \mu_1$ and so $0 \leq \lambda \leq 1$.

Any surface on which $\tau = \tau_y$ which separates yielded and unyielded regions is called a "yield surface". The familiar case of a Newtonian fluid with constant viscosity $\mu_1 = \mu_2$ is recovered in the case $\lambda = 1$ and the Bingham model is recovered in the limit $\lambda \to 0$. In the special case $\tau_y = 0$ the fluid is always yielded and behaves like a Newtonian fluid with constant viscosity μ_2, while in the limit $\tau_y \to \infty$ it is always unyielded and behaves like a Newtonian fluid with constant viscosity μ_1.

3 Problem Formulation

3.1 Flow Down a Planar Substrate

Consider initially the steady unidirectional flow of a thin symmetric rivulet of the biviscosity fluid described in Sec. 2 with prescribed positive volume flux $\bar{Q} > 0$ down a planar substrate inclined at an angle α ($0 \leq \alpha \leq \pi$) to the horizontal, shown in Fig. 2. We choose Cartesian axes $Oxyz$ as indicated in Fig. 2, with the x axis in the direction of flow and the y axis horizontal (transverse to the direction of flow) with respect to which the substrate is denoted by $z = 0$. The fluid velocity and pressure are denoted by $\mathbf{u} = u(y,z)\mathbf{i}$ and $p = p(x,y,z)$ respectively. Provided that $\lambda \neq 0$, the fluid adjacent to the free surface is always unyielded (since the stress is small there) and so in general the solution comprises a region of yielded fluid (region 2), occupying $0 \leq z < H$ for $|y| < b$, and a region of unyielded fluid (region 1) occupying $H \leq z \leq h$ for $|y| < b$ and $0 \leq z \leq h$ for $b \leq |y| \leq a$, where $z = h(y)$ and $z = H(y)$ ($\leq h$) denote the positions of the free surface and of the yield surface respectively and the constants a and b ($\leq a$) denote the semi-widths of the rivulet and the yielded region respectively. We use the subscripts 1 and 2 on u and p to distinguish between quantities in the two regions. Since the rivulet is thin (with, in particular, the prescribed constant contact angle between the free surface and the substrate β satisfying $\beta \ll 1$) employing the familiar lubrication approximation (see, for example, Acheson [21] or Ockendon and Ockendon [22])

the governing equations in the two regions are simply

$$0 = -p_{i,x} + \rho g \sin\alpha + \mu_i u_{i,zz}, \tag{4}$$

$$0 = -p_{i,y}, \tag{5}$$

$$0 = -p_{i,z} - \rho g \cos\alpha, \tag{6}$$

for $i = 1, 2$, subject to the boundary conditions of no slip at the substrate $z = 0$,

$$u_1 = 0 \quad \text{for} \quad b \leq |y| \leq a, \tag{7}$$

$$u_2 = 0 \quad \text{for} \quad |y| < b, \tag{8}$$

continuity of velocity and normal and tangential stress at the yield surface $z = H(y)$,

$$u_1 = u_2, \tag{9}$$

$$p_1 = p_2, \tag{10}$$

$$\mu_1 u_{1,z} = \mu_2 u_{2,z} + \tau_0 = \tau_y, \tag{11}$$

and balances of normal and tangential stress at the free surface $z = h(y)$,

$$p_1 - p_0 = -\gamma h'', \tag{12}$$

$$u_{1,z} = 0, \tag{13}$$

together with the definition of the (unknown) positions of the edges of the yielded region $y = \pm b$,

$$H = 0, \tag{14}$$

and prescribed constant contact angle at the (unknown) positions of the edges of the rivulet $y = \pm a$,

$$h = 0, \tag{15}$$

$$h' = \mp\beta. \tag{16}$$

Here p_0 denotes the constant pressure of the surrounding atmosphere, γ the constant coefficient of surface tension, and g the acceleration due to gravity, while primes denote differentiation with respect to argument. Note that, since the flow is unidirectional, the kinematic condition is identically satisfied.

The present analysis is concerned with small-scale flows, such as those found in many industrial coating and printing processes, whose transverse length scales are of the order of the capillary length $l = (\gamma/\rho g)^{1/2}$, typically 1 cm or less. Yield-stress effects are significant when the thickness of the rivulet is greater than or equal to the yield height $\tau_y/\rho g \sin\alpha$, i.e. when the yield stress is of the order of 10^2 Pa or less. This condition is satisfied for many of the foodstuffs, paints and inks used in industrial coating and printing applications. For simplicity we non-dimensionalise using the capillary length l as the length scale in the y direction, $l\beta$ as the length scale in the z direction, $\gamma\beta^2/\mu_2$ as the velocity scale, and $\rho g l\beta$ as the stress scale. Hereafter all quantities will be non-dimensional unless stated otherwise.

When region 2 is present integrating (6) with $i = 1$ and $i = 2$ respectively subject to (10) on $z = H$ and (12) on $z = h$ yields $p_1 = p$ in $b \le |y| \le a$ and $p_1 = p_2 = p$ in $|y| < b$, where

$$p = p_0 + (h - z)\cos\alpha - h''. \tag{17}$$

Then (5) yields a third-order ordinary differential equation for h, namely

$$h''' = h' \cos\alpha, \tag{18}$$

to be integrated subject to (15) and (16) at $y = \pm a$, and so

$$h(y) = \begin{cases} \dfrac{\cosh ma - \cosh my}{m \sinh ma} & \text{if} \quad 0 \le \alpha < \pi/2, \\ \dfrac{a^2 - y^2}{2a} & \text{if} \quad \alpha = \pi/2, \\ \dfrac{\cos my - \cos ma}{m \sin ma} & \text{if} \quad \pi/2 < \alpha \le \pi, \end{cases} \tag{19}$$

where we have introduced the notation $m = |\cos\alpha|^{1/2}$. From (17) we have $p_x = 0$ and so when

$b \le |y| \le a$ integrating (4) with $i = 1$ subject to (7) on $z = 0$ and (13) on $z = h$ yields

$$u_1 = \frac{\lambda \sin\alpha}{2}(2hz - z^2), \tag{20}$$

but when $|y| < b$ integrating (4) with $i = 1$ and $i = 2$ subject to (8) on $z = 0$, (9) and (11) on $z = H$ and (13) on $z = h$ yields

$$u_1 = \frac{\lambda \sin\alpha}{2}(2hz - z^2 - 2hH + H^2) + \frac{\sin\alpha}{2}(2hH - H^2) - (1-\lambda)\tau_y H, \tag{21}$$

$$u_2 = \frac{\sin\alpha}{2}(2hz - z^2) - (1-\lambda)\tau_y z. \tag{22}$$

The requirement that the stress takes its yield value τ_y on the yield surface $z = H$ means that H is given by

$$H = h - \frac{\tau_y}{\sin\alpha}, \tag{23}$$

showing that the yield surface (when it exists) always lies below the free surface by a constant amount equal to the "yield height" $\tau_y / \sin\alpha$, as indicated in Fig. 2. The volume flux of fluid down the substrate, Q, is given by

$$Q = 2\int_b^a \int_0^h u_1(y,z)\,\mathrm{d}z\,\mathrm{d}y + 2\int_0^b \int_0^H u_2(y,z)\,\mathrm{d}z\,\mathrm{d}y + 2\int_0^b \int_H^h u_1(y,z)\,\mathrm{d}z\,\mathrm{d}y, \tag{24}$$

and so using (20), (21) and (22) together with (23) to eliminate H we obtain

$$\begin{aligned} Q = {} & \frac{2\lambda \sin\alpha}{3}\int_0^a h(y)^3\,\mathrm{d}y + \frac{2(1-\lambda)\sin\alpha}{3}\int_0^b h(y)^3\,\mathrm{d}y \\ & - (1-\lambda)\tau_y \int_0^b h(y)^2\,\mathrm{d}y + \frac{b(1-\lambda)\tau_y^3}{3\sin^2\alpha}. \end{aligned} \tag{25}$$

With (19) and (23) the value of b is determined from (14) at $y = \pm b$ to be

$$b = \begin{cases} \dfrac{1}{m}\cosh^{-1}\left[\cosh ma - \dfrac{m\tau_y}{\sin\alpha}\sinh ma\right] & \text{if} \quad 0 \le \alpha < \pi/2, \\ (a^2 - 2a\tau_y)^{1/2} & \text{if} \quad \alpha = \pi/2, \\ \dfrac{1}{m}\cos^{-1}\left[\cos ma + \dfrac{m\tau_y}{\sin\alpha}\sin ma\right] & \text{if} \quad \pi/2 < \alpha \le \pi. \end{cases} \tag{26}$$

The explicit expression for Q is obtained by substituting for h from (19) into (25). In general this expression is lengthy and so will be omitted for the sake of brevity. In the special case $\alpha = \pi/2$ Eq. (25) (with (26)) simplifies to

$$Q = \frac{4\lambda a^4}{105} + \frac{2(1-\lambda)b^5}{105a^2}(2a + 3\tau_y). \tag{27}$$

When region 2 is absent (in which case the fluid is unyielded everywhere and behaves like a Newtonian fluid with constant dimensional viscosity μ_1) similar arguments yield $p_1 = p$ (i.e. the pressure is given by (17) throughout the flow) and show that h once again satisfies (18) for all y and hence is again given by (19). The velocity u_1 is again given by (20) and Q is now given by

$$Q = 2\int_0^a \int_0^h u_1(y,z)\,\mathrm{d}z\,\mathrm{d}y = \frac{2\lambda \sin\alpha}{3}\int_0^a h(y)^3\,\mathrm{d}y, \tag{28}$$

and so using (19) we obtain

$$Q = \frac{\lambda \sin\alpha}{9m^4} F(ma), \tag{29}$$

where we have defined

$$F(ma) = \begin{cases} 15ma\coth^3 ma - 15\coth^2 ma - 9ma\coth ma + 4 & \text{if} \quad 0 \le \alpha < \pi/2, \\ \dfrac{12}{35}(ma)^4 & \text{if} \quad \alpha = \pi/2, \\ -15ma\cot^3 ma + 15\cot^2 ma - 9ma\cot ma + 4 & \text{if} \quad \pi/2 < \alpha \le \pi, \end{cases} \tag{30}$$

in agreement with the corresponding results obtained by Duffy and Moffatt [10] in the Newtonian case. (Note that in the case $\alpha = \pi/2$ we have $m = 0$ and the factors of m^4 must be cancelled before setting $\alpha = \pi/2$.)

For any prescribed positive value of the volume flux, $\bar{Q} > 0$, the possible rivulet semi-widths are the positive solutions for a of the equation $Q = \bar{Q}$, where Q is given either by (25) if region 2 is present or by (29) if region 2 is absent. Once a is known h, H and b are given by (19), (23) and (26) respectively. From (19) the maximum thickness of the cross section of the rivulet,

denoted by $h_{\rm m} = h(0)$, is given by

$$h_{\rm m} = \begin{cases} \dfrac{1}{m}\tanh\left(\dfrac{ma}{2}\right) & \text{if} \quad 0 \leq \alpha < \pi/2, \\ \dfrac{a}{2} & \text{if} \quad \alpha = \pi/2, \\ \dfrac{1}{m}\tan\left(\dfrac{ma}{2}\right) & \text{if} \quad \pi/2 < \alpha \leq \pi, \end{cases} \tag{31}$$

and from (23) the maximum thickness of the cross section of the yielded region, denoted by $H_{\rm m} = H(0)$, is given by

$$H_{\rm m} = h_{\rm m} - \frac{\tau_{\rm y}}{\sin\alpha}. \tag{32}$$

In practice since the algebra required to calculate Q is rather lengthy we used the symbolic algebra package MAPLE V running on a SUN ULTRA 10 to perform the analytical evaluation of Q from (25) and (29) as well as the subsequent numerical calculation of a from the equation $Q = \bar{Q}$.

3.2 Flow Down a Slowly Varying Substrate

So far the analysis has been restricted to strictly unidirectional flow but, as Duffy and Moffatt [10] describe, this solution is also the leading-order approximation to the local behaviour of a rivulet with non-uniform width draining down a non-planar cylindrical substrate, where α now represents the *local* inclination of the substrate to the horizontal, provided that α varies sufficiently slowly, i.e. provided that both the longitudinal aspect ratio $\epsilon = l\beta/R$ and the reduced Reynolds number $\rho\gamma l^2\beta^4/\mu_2^2 R$ (where R is a typical radius of curvature of the substrate) are sufficiently small. Thus we shall interpret the results given subsequently as describing a slowly varying rivulet draining in the azimuthal direction from the top ($\alpha = 0$) to the bottom ($\alpha = \pi$) of a large horizontal circular cylinder as sketched in Fig. 3. As Wilson and Duffy [12] showed, in the Newtonian case there are multiple branches of solutions for a in $\pi/2 < \alpha \leq \pi$, but of these only the one that connects smoothly with the solution in $0 \leq \alpha < \pi/2$ is physically realisable. We shall henceforth restrict our attention to this latter type of solution. We define

the term "yielded zone" to correspond to those values of α at which region 2 is present; at other values of α (the "unyielded zone") region 2 is absent, the flow is unyielded all the way from $y = -a$ to $y = a$, and the solution is independent of τ_y.

3.3 The Yield Condition

Provided that $\tau_y \neq 0$, for sufficiently small values of $\bar{Q}$ the unyielded zone extends all the way from $\alpha = 0$ to $\alpha = \pi$ and so Q is given by (29) for all $0 \leq \alpha \leq \pi$. However, for sufficiently large values of $\bar{Q}$ a yielded zone is present. The edges of the yielded zone are where $b = 0$, and from (26) we find that the corresponding values of a, denoted by a_y, are given by

$$a_y = \begin{cases} \dfrac{2}{m}\tanh^{-1}\left(\dfrac{m\tau_y}{\sin\alpha}\right) & \text{if} \quad 0 \leq \alpha < \pi/2, \\ 2\tau_y & \text{if} \quad \alpha = \pi/2, \\ \dfrac{2}{m}\tan^{-1}\left(\dfrac{m\tau_y}{\sin\alpha}\right) & \text{if} \quad \pi/2 < \alpha \leq \pi. \end{cases} \tag{33}$$

Substituting $a = a_y$ into (29) yields $Q = Q_y$, where Q_y is given by

$$Q_y = \frac{\lambda \sin\alpha}{9m^4} F(ma_y). \tag{34}$$

The real solutions for α of the equation $Q_y = \bar{Q}$ (if they exist) are the edges of the yielded zone. Figure 4 shows Q_y/λ defined by (34) plotted as a function of α/π for a range of values of τ_y. As Fig. 4 illustrates, Q_y/λ is a concave function of α defined over the interval $\alpha_0 < \alpha < \pi$, where $\alpha_0 = \alpha_0(\tau_y)$ $(0 < \alpha_0 < \pi/2)$ is the solution for α of $m\tau_y = \sin\alpha$, and so

$$\alpha_0 = \cos^{-1}\left[\frac{(\tau_y^4 + 4)^{1/2} - \tau_y^2}{2}\right]. \tag{35}$$

Note that α_0 is a monotonically increasing function of τ_y satisfying $\alpha_0 = \tau_y + O(\tau_y^3)$ as $\tau_y \to 0$, and $\alpha_0 = \pi/2 - \tau_y^{-2} + O(\tau_y^{-6})$ as $\tau_y \to \infty$. As Fig. 4 also shows, Q_y/λ becomes unbounded as $\alpha \to \alpha_0^+$ and as $\alpha \to \pi^-$; also Q_y/λ is decreasing with slope $-256\tau_y^6/945 < 0$ at $\alpha = \pi/2$ where it takes the value $64\tau_y^4/105$, and has a single global minimum value of Q_c/λ (say) at

$\alpha = \alpha_c$, where $\alpha_c = \alpha_c(\tau_y)$ $(\pi/2 < \alpha_c < \pi)$ is the solution for α of

$$2(1+\sin^2\alpha)F(ma_y) = (1+\cos^2\alpha)F'(ma_y)\sin ma_y, \tag{36}$$

where F and a_y are given by (30) and (33) respectively. Local analysis of (36) reveals that as $\tau_y \to 0$ we have

$$\alpha_c \sim \frac{\pi}{2} + \frac{4\tau_y^2}{27}, \quad Q_c \sim \frac{64\lambda\tau_y^4}{105}, \tag{37}$$

and as $\tau_y \to \infty$ we have

$$\alpha_c \sim \pi - \tan^{-1}2 - \frac{36\sqrt{5}}{125\tau_y^2}, \quad Q_c \sim \frac{5^{9/4}\pi\lambda\tau_y^3}{96}, \tag{38}$$

where $\pi - \tan^{-1}2 \simeq 0.6475\pi$. Figure 5(a) shows α_0/π given by (35) and α_c/π obtained from (36) plotted as functions of τ_y. Figure 5(b) shows Q_c/λ also plotted as a function of τ_y. Figure 5 also shows the corresponding leading-order asymptotic expressions for α_c/π and Q_c/λ in the limits $\tau_y \to 0$ and $\tau_y \to \infty$ given by (37) and (38). In particular, Fig. 5 shows that both α_c and Q_c are monotonically increasing functions of τ_y. Thus for $\bar{Q} < Q_c$ (or equivalently $\tau_y > \tau_{yc}$, where τ_{yc} is the value of τ_y for which $Q_c = \bar{Q}$) Eq. (34) has no real roots for α and so the unyielded zone extends all the way from $\alpha = 0$ to $\alpha = \pi$. On the other hand, for $\bar{Q} > Q_c$ (or equivalently $\tau_y < \tau_{yc}$) Eq. (34) has two distinct real roots denoted by α_1 and α_2, where $\alpha_0 \le \alpha_1 < \alpha_c < \alpha_2 \le \pi$, and so the flow comprises a yielded zone $\alpha_1 < \alpha < \alpha_2$, an "upper unyielded zone" $0 \le \alpha \le \alpha_1$ and a "lower unyielded zone" $\alpha_2 \le \alpha \le \pi$. For $Q_c < \bar{Q} < 64\lambda\tau_y^4/105$ we have $\pi/2 < \alpha_1 < \alpha_c$ and the yielded zone is confined to the lower half of the cylinder, but for $\bar{Q} > 64\lambda\tau_y^4/105$ we have $\alpha_0 < \alpha_1 < \pi/2$ and the yielded zone extends over $\alpha = \pi/2$ into the upper half of the cylinder.

Local analysis of (25) and (29) near $\alpha = \alpha_1$ and $\alpha = \alpha_2$ shows that a, $\mathrm{d}a/\mathrm{d}\alpha$, h_m and $\mathrm{d}h_m/\mathrm{d}\alpha$ are continuous at $\alpha = \alpha_1$ and $\alpha = \alpha_2$, and that $b = O(\alpha-\alpha_1)^{1/2}$ and $H_m = O(\alpha-\alpha_1)$ as $\alpha \to \alpha_1^+$, and $b = O(\alpha_2-\alpha)^{1/2}$ and $H_m = O(\alpha_2-\alpha)$ as $\alpha \to \alpha_2^-$; in particular $|\mathrm{d}b/\mathrm{d}\alpha| \to \infty$ but $|\mathrm{d}H_m/\mathrm{d}\alpha|$ remains finite in these limits.

Figure 6 shows typical solutions for a, b, $h_{\rm m}$ and $H_{\rm m}$ which demonstrate the features described above. In particular, Fig. 6(a) shows a and b, the semi-widths of the rivulet and of the yielded region, plotted as functions of α/π in the case $\tau_{\rm y} = 1$, $\bar{Q} = 1$ and $\lambda = 1/2$, and Fig. 6(b) shows the corresponding values of $h_{\rm m}$ and $H_{\rm m}$, the maximum thicknesses of the rivulet and of the yielded region, also plotted as functions of α/π. Note that in this case $\alpha_1/\pi \simeq 0.3141$ and $\alpha_2/\pi \simeq 0.8155$. Figure 7 shows the corresponding transverse profiles of the free surface $z = h(y)$ and (when present) of the yield surface $z = H(y)$ for a range of values of α.

Of course this analysis also applies to unidirectional flow with flux $\bar{Q}$ down a planar substrate inclined at an angle α to the horizontal. If $0 \leq \alpha \leq \alpha_0$ then the fluid is entirely unyielded, while if $\alpha_0 < \alpha \leq \pi$ then the fluid is entirely unyielded if $\bar{Q} \leq Q_{\rm y}$ but has a yielded region if $\bar{Q} > Q_{\rm y}$ (and hence, in particular, the fluid is entirely unyielded when $\bar{Q} \leq Q_{\rm c}$).

4 Results

Before analysing the behaviour of the solution in appropriate asymptotic limits it is useful to note the following results for future reference. If $a \to \infty$ in $0 \leq \alpha < \pi/2$ then from (19)

$$h \sim \frac{1}{m}\left[1 - e^{-m(a-y)}\right]. \tag{39}$$

Thus in $0 \leq \alpha \leq \min(\alpha_1, \pi/2)$ we find from (28) that

$$Q \sim \frac{2\lambda \sin\alpha}{3m^3} a, \tag{40}$$

and if $\alpha_1 < \pi/2$ then in $\alpha_1 < \alpha < \pi/2$ we find from (26) that $b \to \infty$ with

$$a - b \sim -\frac{1}{m} \log\left[1 - \frac{m\tau_{\rm y}}{\sin\alpha}\right] \tag{41}$$

and from (25) that

$$Q \sim \left[\frac{2\sin\alpha}{3m^3} - \frac{(1-\lambda)\tau_{\rm y}}{m^2} + \frac{(1-\lambda)\tau_{\rm y}^3}{3\sin^2\alpha}\right] a. \tag{42}$$

Also, if $ma \to \pi$ in $\pi/2 < \alpha \leq \pi$ then from (19)

$$h \sim \frac{1+\cos my}{m(\pi - ma)}. \tag{43}$$

Thus in $\alpha_2 \leq \alpha \leq \pi$ and if $\alpha_1 > \pi/2$ then in $\pi/2 < \alpha \leq \alpha_1$ we find from (28) that

$$Q \sim \frac{5\pi\lambda \sin\alpha}{3m^4(\pi - ma)^3}, \tag{44}$$

and in $\max(\alpha_1, \pi/2) < \alpha < \alpha_2$ we find from (26) that $mb \to \pi$ and from (25) that

$$Q \sim \frac{5\pi \sin\alpha}{3m^4(\pi - ma)^3}. \tag{45}$$

4.1 The Limits $\alpha \to 0^+$ and $\alpha \to \pi^-$

Provided that $\tau_y \neq 0$ the flow is always unyielded near $\alpha = 0$ and, except in the special case $\lambda = 0$ discussed subsequently in Sec. 4.5, near $\alpha = \pi$, and so from (29) as $\alpha \to 0^+$ we have

$$a \sim \frac{3\bar{Q}}{2\lambda\alpha}, \quad h_m \sim 1 + \frac{\alpha^2}{4} \tag{46}$$

(so that, in particular, the rivulet becomes infinitely wide in the transverse direction with uniform thickness unity), and as $\alpha \to \pi^-$ we have

$$a \sim \pi - \left[\frac{5\pi\lambda(\pi-\alpha)}{3\bar{Q}}\right]^{1/3}, \quad h_m \sim \left[\frac{24\bar{Q}}{5\pi\lambda(\pi-\alpha)}\right]^{1/3} \tag{47}$$

(so that, in particular, the rivulet becomes infinitely thick with semi-width π), in agreement with the results of Duffy and Moffatt [10] in the Newtonian case. Note that (20) gives $u_1 = O(\alpha)$ as $\alpha \to 0^+$ and $u_1 = O(\pi - \alpha)$ as $\alpha \to \pi^-$ so that the flow is slow and hence the flux remains $O(1)$ in both limits, as it should. It should, however, be noted that the lubrication approximation breaks down as $\alpha \to \pi^-$.

4.2 Varying τ_y

Figure 8 shows a, b, h_m and H_m plotted as functions of α/π for a range of values of τ_y in the case $\bar{Q} = 1$ and $\lambda = 1/2$. In particular, Fig. 8 includes the solutions in the special case $\tau_y = 0$

in which the flow is yielded everywhere with $a = b$, $h_{\rm m} = H_{\rm m}$, $\alpha_1 = 0$ and $\alpha_2 = \pi$. In this case the fluid behaves like a Newtonian fluid with constant dimensional viscosity μ_2, and hence the entirely yielded solution in this case is identical to the corresponding entirely unyielded solution with λ set to unity. In particular, this means that when $\tau_{\rm y} = 0$ the asymptotic behaviours of $a = b$ and $h_{\rm m} = H_{\rm m}$ in the limits $\alpha \to 0^+$ and $\alpha \to \pi^-$ are given by (46) and (47) with $\lambda = 1$ respectively. Figure 8 also illustrates that the solution in the unyielded zone is independent of $\tau_{\rm y}$. In particular, for $\tau_{\rm y} \geq \tau_{\rm yc}$ (where in this case $\tau_{\rm yc} \simeq 1.3763$) the flow is unyielded everywhere and the fluid behaves like a Newtonian fluid with constant dimensional viscosity μ_1.

4.3 Varying $\bar{Q}$

Figure 9 shows a, b, $h_{\rm m}$ and $H_{\rm m}$ plotted as functions of α/π for a range of values of $\bar{Q}$ in the case $\tau_{\rm y} = 1$ and $\lambda = 1/2$, for which $Q_{\rm c} \simeq 0.2958$ and $\alpha_{\rm c}/\pi \simeq 0.5435$.

In the limit of small flux $\bar{Q} \to 0$ the flow is unyielded everywhere and we have

$$a \sim \left(\frac{105\bar{Q}}{4\lambda \sin\alpha}\right)^{1/4}, \quad h_{\rm m} \sim \frac{1}{2}\left(\frac{105\bar{Q}}{4\lambda \sin\alpha}\right)^{1/4}, \tag{48}$$

in agreement with the corresponding results of Holland, Duffy and Wilson [13] in the Newtonian case.

In the limit of large flux $\bar{Q} \to \infty$ we have $\alpha_1 \to \alpha_0^+$ (where $0 < \alpha_0 < \pi/2$) and $\alpha_2 \to \pi^-$ according to

$$\alpha_1 \sim \alpha_0 + \frac{4\sin\alpha_0\cos\alpha_0}{1+\cos^2\alpha_0}\exp\left[-\frac{3\bar{Q}\cos^2\alpha_0}{2\lambda\sin\alpha_0}\right] \tag{49}$$

and

$$\alpha_2 \sim \pi - \left[\frac{5\pi\lambda\tau_{\rm y}^3}{24\bar{Q}}\right]^{1/2}. \tag{50}$$

In the upper unyielded zone $0 \leq \alpha \leq \alpha_1$ we find from (29) that

$$a \sim \frac{3\bar{Q}(\cos\alpha)^{3/2}}{2\lambda\sin\alpha} + \frac{11}{6(\cos\alpha)^{1/2}}, \tag{51}$$

and so from (31)

$$h_{\mathrm{m}} \sim \frac{1}{(\cos\alpha)^{1/2}}, \tag{52}$$

while in the lower unyielded zone $\alpha_2 \leq \alpha \leq \pi$ we find from (29) and (31) that a and h_{m} are given by (47). The behaviour in the yielded zone $\alpha_1 < \alpha < \alpha_2$ is different depending on whether $\alpha < \pi/2$ or $\alpha > \pi/2$. In $\alpha_1 < \alpha < \pi/2$ from (42)

$$a,\, b \sim \left[\frac{2\sin\alpha}{3(\cos\alpha)^{3/2}} - \frac{(1-\lambda)\tau_{\mathrm{y}}}{\cos\alpha} + \frac{(1-\lambda)\tau_{\mathrm{y}}^3}{3\sin^2\alpha}\right]^{-1} \bar{Q}, \tag{53}$$

with $a - b = O(1)$ according to (41), and so from (31) and (32)

$$h_{\mathrm{m}} \sim \frac{1}{(\cos\alpha)^{1/2}}, \quad H_{\mathrm{m}} \sim \frac{1}{(\cos\alpha)^{1/2}} - \frac{\tau_{\mathrm{y}}}{\sin\alpha}, \tag{54}$$

while in $\pi/2 < \alpha < \alpha_2$ from (45)

$$a \sim \frac{\pi}{|\cos\alpha|^{1/2}} - \left[\frac{5\pi\sin\alpha}{3\bar{Q}}\right]^{1/3} \frac{1}{|\cos\alpha|^{7/6}}, \tag{55}$$

$$b \sim \frac{\pi}{|\cos\alpha|^{1/2}} - \left[\frac{40\pi\tau_{\mathrm{y}}^3}{3\bar{Q}\sin^2\alpha}\right]^{1/6} \frac{1}{|\cos\alpha|^{7/12}}, \tag{56}$$

and so from (31) and (32)

$$h_{\mathrm{m}},\, H_{\mathrm{m}} \sim \left[\frac{24\bar{Q}}{5\pi\sin\alpha}\right]^{1/3} |\cos\alpha|^{1/6}. \tag{57}$$

At $\alpha = \pi/2$ the fluid is unyielded and from (26) and (27)

$$a,\, b \sim \left(\frac{105\bar{Q}}{4}\right)^{1/4}, \tag{58}$$

with $a - b \sim \tau_{\mathrm{y}}$, and so from (31) and (32)

$$h_{\mathrm{m}}, H_{\mathrm{m}} \sim \frac{1}{2}\left(\frac{105\bar{Q}}{4}\right)^{1/4}. \tag{59}$$

Note that a, $\mathrm{d}a/\mathrm{d}\alpha$, h_{m} and $\mathrm{d}h_{\mathrm{m}}/\mathrm{d}\alpha$ are continuous at $\alpha = \alpha_1$ and $\alpha = \alpha_2$.

Thus, when $\bar{Q} \to \infty$, in $0 \leq \alpha < \pi/2$ we have $a = O(\bar{Q})$ and $h_{\mathrm{m}} = O(1)$ (together with $b = O(\bar{Q})$ and $H_{\mathrm{m}} = O(1)$ in $\alpha_1 < \alpha < \pi/2$) while in $\pi/2 < \alpha \leq \pi$ we have $a = O(1)$

and $h_m = O(\bar{Q}^{1/3})$ (together with $b = O(1)$ and $H_m = O(\bar{Q}^{1/3})$ in $\pi/2 < \alpha < \alpha_2$). The adjustments between these two different types of asymptotic behaviour occur via boundary layers of thickness $O(\bar{Q}^{-1/2})$ near $\alpha = \pi/2$ where a, b, h_m and H_m are $O(\bar{Q}^{1/4})$. In the special case $\lambda = 1$ these results reduce to those of Holland, Duffy and Wilson [13] in the Newtonian case.

4.4 Varying λ

Figure 10 shows a, b, h_m and H_m plotted as functions of α/π for a range of values of λ including $\lambda = 0$ in the case $\tau_y = 1$ and $\bar{Q} = 1$, for which there is always a yielded zone.

In the special case $\lambda = 1$ we recover the results for a Newtonian fluid with constant dimensional viscosity $\mu_1 = \mu_2$. In this case the yield surface H (when present) is merely the surface on which the stress takes the yield value τ_y but across which the fluid undergoes no material change.

In the Bingham limit $\lambda \to 0$ it is found that $\alpha_1 \to \alpha_0^+$ and $\alpha_2 \to \pi^-$ according to (49) and (50) respectively. In the upper unyielded zone $0 \leq \alpha \leq \alpha_1$ we have $a = O(\lambda^{-1})$ and $h_m = O(1)$ according to (51) and (52), while in the lower unyielded zone $\alpha_2 \leq \alpha \leq \pi$ we have $a = O(1)$ and $h_m = O(\lambda^{-1/3})$ according to (47). At $\alpha = \pi/2$ we find that a, b, h_m and H_m are $O(1)$. The solution in the special case $\lambda = 0$ is discussed in detail in the next section.

4.5 The Special Case $\lambda = 0$

The solution in the special case $\lambda = 0$ in which $\alpha_1 = \alpha_0$ and $\alpha_2 = \pi$ is of particular interest. In this case the solution in the upper unyielded zone ($0 \leq \alpha \leq \alpha_0$) is an infinitely wide rigid and stationary plug of uniform thickness $(\cos\alpha)^{-1/2}$ and the lower unyielded zone is absent. In the yielded zone ($\alpha_0 < \alpha \leq \pi$) the flow is rather more complicated. Substituting $\lambda = 0$ into (20) yields $u_1 = 0$ when $b \leq |y| \leq a$ showing that $-a \leq y \leq -b$ and $b \leq y \leq a$ are two stationary "levées" of rigid unyielded material of the kind first suggested by Hulme [17] in the

geophysical (large-scale) context. Substituting $\lambda = 0$ into (21), (22) and (25) and simplifying using (23) yields

$$u_1 = \frac{\sin\alpha}{2} H^2, \tag{60}$$

$$u_2 = \frac{\sin\alpha}{2}(2Hz - z^2), \tag{61}$$

$$Q = \frac{2\sin\alpha}{3}\int_0^b H(y)^3\,\mathrm{d}y + \tau_y \int_0^b H(y)^2\,\mathrm{d}y \tag{62}$$

when $|y| < b$. In particular, (60) and (61) show that whereas region 2 is "fully plastic", region 1 is a "pseudo-plug" whose velocity u_1 is independent of z (but not y or α) and in which the stress is significantly below the yield stress. The geometry of the locally unidirectional solution in the yielded zone when $\lambda = 0$ is shown in Fig. 11. Again this analysis also applies to unidirectional flow with flux $\bar{Q}$ down a planar substrate inclined at an angle α to the horizontal, for which there is no flow for $0 \leq \alpha \leq \alpha_0$, while for $\alpha_0 < \alpha \leq \pi$ the flow is as shown in Fig. 11.

As Fig. 10 illustrates, some aspects of the behaviour of the solution in the special case $\lambda = 0$ are qualitatively different from those in the general case $\lambda \neq 0$ described previously. In particular, the asymptotic behaviours of a, b, h_m and H_m in the limits $\alpha \to \alpha_1^+ = \alpha_0^+$ and $\alpha \to \alpha_2^- = \pi^-$ when $\lambda = 0$ are somewhat different from those when $\lambda \neq 0$. Specifically we find that as $\alpha \to \alpha_0^+$

$$a,\, b \;\sim\; \left[\frac{2\cos\alpha_0}{2\cos\alpha_0 + \tau_y^2}\right]^2 \frac{\bar{Q}\tau_y}{(\alpha - \alpha_0)^2}, \tag{63}$$

$$h_m \;\sim\; \frac{1}{(\cos\alpha_0)^{1/2}} + \frac{\tau_y}{2\cos\alpha_0}(\alpha - \alpha_0), \tag{64}$$

$$H_m \;\sim\; \left[\frac{2\cos\alpha_0 + \tau_y^2}{2\tau_y\cos\alpha_0}\right](\alpha - \alpha_0) \tag{65}$$

(so that, in particular, the yielded region becomes infinitely wide in the transverse direction), and as $\alpha \to \pi^-$

$$a \;\sim\; \pi - \frac{2}{\tau_y}(\pi - \alpha) + \left[\frac{225\bar{Q}^2}{8\tau_y^{11}}\right]^{1/5}(\pi - \alpha)^{9/5}, \tag{66}$$

$$b \sim \left[\frac{30\bar{Q}}{\tau_y^3}\right]^{1/5}(\pi-\alpha)^{2/5}, \tag{67}$$

$$h_m \sim \frac{\tau_y}{\pi-\alpha}+\frac{1}{2}\left[\frac{225\bar{Q}^2}{8\tau_y}\right]^{1/5}(\pi-\alpha)^{-1/5}, \tag{68}$$

$$H_m \sim \frac{1}{2}\left[\frac{225\bar{Q}^2}{8\tau_y}\right]^{1/5}(\pi-\alpha)^{-1/5} \tag{69}$$

(so that, in particular, the yielded region becomes infinitely thick).

Figures 12 and 13 show a, b, h_m and H_m plotted as functions of α/π when $\lambda = 0$ for a range of values of τ_y when $\bar{Q} = 1$ and a range of values of $\bar{Q}$ when $\tau_y = 1$, respectively.

As Fig. 12 illustrates, in the limit $\tau_y \to 0$ we have $\alpha_0 \to 0^+$ and the behaviour when $\lambda = 0$ is the same as that when $\lambda \neq 0$, i.e. the fluid behaves like a Newtonian fluid with constant dimensional viscosity μ_2, and hence the entirely yielded solution in this case is identical to the corresponding entirely unyielded solution with λ set to unity. On the other hand, in the limit $\tau_y \to \infty$ we have $\alpha_0 \to \pi/2^-$ and the behaviour when $\lambda = 0$ is qualitatively different from that when $\lambda \neq 0$. Specifically as $\tau_y \to \infty$

$$a \sim \frac{\pi}{|\cos\alpha|^{1/2}}-\frac{2\sin\alpha}{|\cos\alpha|\,\tau_y}+\left[\frac{225\bar{Q}^2\sin^9\alpha}{8\cos^4\alpha\,\tau_y^{11}}\right]^{1/5}, \tag{70}$$

$$b \sim \left[\frac{30\bar{Q}\tan^2\alpha}{\tau_y^3}\right]^{1/5}, \tag{71}$$

$$h_m \sim \frac{\tau_y}{\sin\alpha}+\frac{1}{2}\left[\frac{225\bar{Q}^2|\cos\alpha|}{8\sin\alpha\,\tau_y}\right]^{1/5}, \tag{72}$$

$$H_m \sim \frac{1}{2}\left[\frac{225\bar{Q}^2|\cos\alpha|}{8\sin\alpha\,\tau_y}\right]^{1/5} \tag{73}$$

for $\pi/2 < \alpha < \pi$.

As Fig. 13 illustrates, in the limit $\bar{Q} \to 0$ the behaviour when $\lambda = 0$ is qualitatively different from that when $\lambda \neq 0$. Specifically as $\bar{Q} \to 0$ if $\alpha_0 < \alpha < \pi/2$ then

$$a \sim a_y + \sin\alpha\left[\frac{225\bar{Q}^2\sinh^4 ma_y}{128m^4\tau_y^7}\right]^{1/5}, \quad b \sim \left[\frac{15\bar{Q}\sinh^2 ma_y}{2m^2\tau_y}\right]^{1/5}, \tag{74}$$

$$h_m \sim \frac{\tau_y}{\sin\alpha}+\left[\frac{225\bar{Q}^2m}{128\tau_y^2\sinh ma_y}\right]^{1/5}, \quad H_m \sim \left[\frac{225\bar{Q}^2m}{128\tau_y^2\sinh ma_y}\right]^{1/5}, \tag{75}$$

if $\alpha = \pi/2$ then

$$a \sim 2\tau_y + \left[\frac{225\bar{Q}^2}{8\tau_y^3}\right]^{1/5}, \quad b \sim [30\bar{Q}\tau_y]^{1/5}, \tag{76}$$

$$h_m \sim \tau_y + \frac{1}{2}\left[\frac{225\bar{Q}^2}{8\tau_y^3}\right]^{1/5}, \quad H_m \sim \frac{1}{2}\left[\frac{225\bar{Q}^2}{8\tau_y^3}\right]^{1/5}, \tag{77}$$

while if $\pi/2 < \alpha < \pi$ then

$$a \sim a_y + \sin\alpha\left[\frac{225\bar{Q}^2 \sin^4 ma_y}{128m^4\tau_y^7}\right]^{1/5}, \quad b \sim \left[\frac{15\bar{Q}\sin^2 ma_y}{2m^2\tau_y}\right]^{1/5}, \tag{78}$$

$$h_m \sim \frac{\tau_y}{\sin\alpha} + \left[\frac{225\bar{Q}^2 m}{128\tau_y^2 \sin ma_y}\right]^{1/5}, \quad H_m \sim \left[\frac{225\bar{Q}^2 m}{128\tau_y^2 \sin ma_y}\right]^{1/5}, \tag{79}$$

where a_y is given by (33). On the other hand, in the limit $\bar{Q} \to \infty$ the behaviour when $\lambda = 0$ is the same as that when $\lambda \neq 0$ described in Sec. 4.3 with λ set to zero.

4.6 Solution for a Bingham Material

The flow of a rivulet of Bingham material (which behaves like a perfectly rigid solid below the yield stress) is of special interest. The Bingham model is recovered from the biviscosity model in the limit $\lambda \to 0$, but the solution for a Bingham material is *not* simply the solution in the case $\lambda = 0$ described in Sec. 4.5 because, as Wilson [5] pointed out, taking the Bingham limit of the thin-film flow of a biviscosity fluid (corresponding to taking the limit $\epsilon \to 0$, where ϵ is the longitudinal aspect ratio of the flow defined in Sec. 3.2, followed by the limit $\lambda \to 0$) is fundamentally different from taking the thin-film limit of flow of a Bingham material (corresponding to taking the limit $\lambda \to 0$ followed by the limit $\epsilon \to 0$). A detailed asymptotic analysis of the thin-film flow of a Bingham material is not attempted here, but comparison with the work of Walton and Bittleston [4], Balmforth and Craster [3], Wilson [5] and Ross, Wilson and Duffy [6] described in Sec. 1 indicates that the solution can be obtained by interpreting the solution for a biviscosity material in the case $\lambda = 0$ described in Sec. 4.5 appropriately. Specifically this work suggests that the yield surface $z = H(y)$ separating region 1 and region 2

should be interpreted as a "pseudo-yield surface" $z = H^*(y)$ separating the pseudo-plug region $H^* \leq z \leq h$ whose velocity is independent of z (but not y or α) and in which the stress is just (specifically $O(\epsilon)$) above the yield stress from the fully plastic region $0 \leq z < H^*$ in which the stress is significantly (specifically $O(1)$) above the yield stress. Presumably an investigation of the distinguished limit $\lambda \to 0$ and $\epsilon \to 0$ with $\lambda/\epsilon = O(1)$ such as that undertaken by Wilson [5] and Ross, Wilson and Duffy [6] would again reveal the location of the true yield surface $z = H(y)$ within the pseudo-plug dividing it into regions in which the stress is either significantly (specifically $O(1)$) below or just (specifically $O(\epsilon)$) above the yield stress, but since physically this detail is of only secondary importance we do not pursue it further here.

It is important to note that, while the velocity in the pseudo-plug region present in the unidirectional axial flow studied by Walton and Bittleston [4] varies only transversely (that is, azimuthally), and the velocities in the pseudo-plug regions present in the non-unidirectional two-dimensional flows studied by Balmforth and Craster [3], Wilson [5] and Ross, Wilson and Duffy [6] vary only longitudinally, the velocity in the pseudo-plug region in the present problem varies with *both* y *and* α. In particular, this means that (unlike in the flows studied by Balmforth and Craster [3], Wilson [5] and Ross, Wilson and Duffy [6] but like in the flow studied by Walton and Bittleston [4]) even in the special case of strictly unidirectional flow down an inclined plane (i.e. the special case in which α is constant) the present solution contains a pseudo-plug region whose velocity varies with y.

5 Conclusions

We used the lubrication approximation to investigate the steady locally unidirectional gravity-driven draining of a thin rivulet of viscoplastic material, modelled as a biviscosity fluid (or, as a special case, as a Bingham material), down a slowly varying substrate. In contrast to the earlier work on viscoplastic rivulets we considered small-scale flows, such as those found in many

industrial coating and printing processes, in which surface-tension effects play a significant role. We interpreted our results as describing a slowly varying rivulet draining in the azimuthal direction from the top to the bottom of a large horizontal circular cylinder. Provided that $\tau_y \neq 0$ we found that the flow is always unyielded near $\alpha = 0$ (where the rivulet becomes infinitely wide in the transverse direction with uniform thickness unity) and, except in the special case $\lambda = 0$, near $\alpha = \pi$ (where it becomes infinitely thick with semi-width π). For $\bar{Q} \leq Q_c$ (or equivalently $\tau_y \geq \tau_{yc}$) the flow is unyielded everywhere, but for $\bar{Q} > Q_c$ (or equivalently $\tau_y < \tau_{yc}$) there is a yielded zone $\alpha_1 < \alpha < \alpha_2$ (where $\alpha_1 \geq \alpha_0$ and $\alpha_2 \leq \pi$) in which the flow near the substrate in the centre of the rivulet is yielded. For $Q_c \leq \bar{Q} < 64\lambda\tau_y^4/105$ the yielded zone is confined to the lower half of the cylinder, but for $\bar{Q} > 64\lambda\tau_y^4/105$ it extends over $\alpha = \pi/2$ into the upper half of the cylinder. We obtained numerically calculated values of a, b, h_m and H_m for a range of parameter values, and described the asymptotic behaviour of the solution in the limits of large and small τ_y, large and small $\bar{Q}$, and small λ. In the special cases $\lambda = 0$ and of a Bingham material we have $\alpha_1 = \alpha_0$ and $\alpha_2 = \pi$, and the flow in the unyielded zone $0 \leq \alpha \leq \alpha_0$ consists of an infinitely wide rigid and stationary plug with uniform thickness $(\cos\alpha)^{-1/2}$, while in the yielded zone $\alpha_0 < \alpha \leq \pi$ it consists of two rigid and stationary "levées" at the edges of the rivulet and a central region in which the flow near the free surface is a pseudo-plug whose velocity is independent of z (but not y or α), separated from the fully plastic flow near the substrate by a pseudo-yield surface. In the case $\lambda = 0$ the stress in the pseudo-plug is significantly below the yield stress, while in the case of a Bingham material it is just above it.

Acknowledgements

The first author (SKW) gratefully acknowledges the ongoing the financial support of the Leverhulme Trust via a Research Fellowship. The third author (ABR) gratefully acknowledges

the financial support of the University of Strathclyde Research and Development Fund.

References

[1] R. B. Bird, G. C. Dai and B. J. Yarusso, "The rheology and flow of viscoplastic materials," Rev. Chem. Eng. **1**, 1 (1983).

[2] H. A. Barnes, "The yield stress — a review or '$\pi\alpha\nu\tau\alpha\ \rho\epsilon\iota$' — everything flows?" J. Non-Newt. Fluid Mech. **81**, 133 (1999).

[3] N. J. Balmforth and R. V. Craster, "A consistent thin-layer theory for Bingham plastics," J. Non-Newt. Fluid Mech. **84**, 65 (1999).

[4] I. C. Walton and S. H. Bittleston, "The axial flow of a Bingham plastic in a narrow eccentric annulus," J. Fluid Mech. **222**, 39 (1991).

[5] S. D. R. Wilson, "A note on thin-layer theory for Bingham plastics," J. Non-Newt. Fluid Mech. **85**, 29 (1999).

[6] A. B. Ross, S. K. Wilson and B. R. Duffy, "Thin-film flow of a viscoplastic material round a large horizontal stationary or rotating cylinder," J. Fluid Mech. **430**, 309 (2001).

[7] G. D. Towell and L. B. Rothfeld, "Hydrodynamics of rivulet flow," AIChE. J. **12**, 972 (1966).

[8] S. Rosenblat, "Rivulet flow of a viscoelastic liquid," J. Non-Newt. Fluid Mech. **13**, 259 (1983).

[9] S. V. Alekseenko, P. I. Geshev and P. A. Kuibin, "Free-boundary fluid flow on an inclined cylinder," Physics - Doklady **42**, 269 (1997).

[10] B. R. Duffy and H. K. Moffatt, "Flow of a viscous trickle on a slowly varying incline," Chem. Eng. J. **60**, 141 (1995).

[11] R. F. Allen and C. M. Biggin, "Longitudinal flow of a lenticular liquid filament down an inclined plane," Phys. Fluids **17**, 287 (1974).

[12] S. K. Wilson and B. R. Duffy, "On the gravity-driven draining of a rivulet of viscous fluid down a slowly varying substrate with variation transverse to the direction of flow," Phys. Fluids **10**, 13 (1998).

[13] D. Holland, B. R. Duffy and S. K. Wilson, "Thermocapillary effects on a thin viscous rivulet draining steadily down a uniformly heated or cooled slowly varying substrate," to appear in J. Fluid Mech. (2001).

[14] P. C. Smith, "A similarity solution for slow viscous flow down an inclined plane," J. Fluid Mech. **58**, 275 (1973).

[15] B. R. Duffy and H. K. Moffatt, "A similarity solution for viscous source flow on a vertical plane," Euro. J. Appl. Math. **8**, 37 (1997).

[16] S. K. Wilson, B. R. Duffy and S. H. Davis, "On a slender dry patch in a liquid film draining under gravity down an inclined plane," to appear in Euro. J. Appl. Math. (2001).

[17] G. Hulme, "The interpretation of lava flow morphology," Geophys. J. R. Astr. Soc. **39** 361 (1974).

[18] P. Coussot and S. Proust, "Slow, unconfined spreading of a mudflow," J. Geophys. Res. **101**, 25217 (1996).

[19] S. D. R. Wilson and S. L. Burgess, "The steady, spreading flow of a rivulet of mud," J. Non-Newt. Fluid Mech. **79**, 77 (1998).

[20] As there is now deformation at low shear rates this special value of the stress should strictly be called a "critical stress" or a "distinguished stress", but we shall use the term "yield stress" for simplicity.

[21] D. J. Acheson, *Elementary Fluid Dynamics* (Oxford University Press, Oxford, United Kingdom, 1990), pp. 238–259.

[22] H. Ockendon and J. R. Ockendon, *Viscous Flow* (Cambridge University Press, Cambridge, United Kingdom, 1995), pp. 64–82.

Figure Captions

FIG. 1 : The biviscosity model.

FIG. 2 : The geometry of the unidirectional flow problem.

FIG. 3 : Sketch of a slowly varying rivulet draining in the azimuthal direction from the top ($\alpha = 0$) to the bottom ($\alpha = \pi$) of a large horizontal cylinder.

FIG. 4 : Q_y/λ given by (34) plotted as a function of α/π for $\tau_y = 1/5,\ 2/5,\ \ldots,\ 8/5$. Each curve is defined on $\alpha_0(\tau_y) < \alpha < \pi$ and has a single global minimum value of $Q_c(\tau_y)/\lambda$ at $\alpha = \alpha_c(\tau_y)$.

FIG. 5 : (a) α_0/π given by (35) and α_c/π obtained from (36), and (b) Q_c/λ plotted as functions of τ_y. The corresponding leading-order asymptotic expressions for α_c/π and Q_c/λ in the limits $\tau_y \to 0$ and $\tau_y \to \infty$ given by (37) and (38) are marked with dashed lines.

FIG. 6 : (a) The semi-width of the rivulet a and of the yielded region b, and (b) the maximum thickness of the rivulet h_m and of the yielded region H_m plotted as functions of α/π in the case $\tau_y = 1$, $\bar{Q} = 1$ and $\lambda = 1/2$. Note that in this case $\alpha_1/\pi \simeq 0.3141$ and $\alpha_2/\pi \simeq 0.8155$.

FIG. 7 : The transverse profiles of the free surface $z = h(y)$ and (when present) of the yield surface $z = H(y)$ plotted as functions of y for (a) $\alpha = \pi/10,\ \pi/5,\ \ldots,\ \pi/2$ and (b) $\alpha = \pi/2,\ 3\pi/5,\ \ldots,\ 9\pi/10$ in the case $\tau_y = 1$, $\bar{Q} = 1$ and $\lambda = 1/2$. For clarity parts (a) and (b) are drawn using different horizontal scales.

FIG. 8 : (a) The semi-width of the rivulet a and of the yielded region b, and (b) the maximum thickness of the rivulet h_m and of the yielded region H_m plotted as functions of α/π for $\tau_y = 0$ (in which case the flow is yielded everywhere), 1/4, 1/2, 3/4, 1 and $\tau_y \geq \tau_{yc} \simeq 1.3763$ (for

which the flow is unyielded everywhere and hence independent of τ_y) in the case $\bar{Q} = 1$ and $\lambda = 1/2$. For clarity the curves in the special case $\tau_y = 0$ (in which $a = b$ and $h_m = H_m$) are marked with dashed lines.

FIG. 9 : (a) The semi-width of the rivulet a and of the yielded region b, and (b) the maximum thickness of the rivulet h_m and of the yielded region H_m plotted as functions of α/π for $\bar{Q} = 1/5$, 1/2, 1, 2, 5 and 10 in the case $\tau_y = 1$ and $\lambda = 1/2$. The leading-order asymptotic values in the limit $\bar{Q} \to \infty$ given by a, $b \sim \pi/|\cos\alpha|^{1/2}$ for $\pi/2 < \alpha \leq \pi$ and by $h_m \sim 1/(\cos\alpha)^{1/2}$ and $H_m \sim 1/(\cos\alpha)^{1/2} - \tau_y/\sin\alpha$ for $0 \leq \alpha < \pi/2$ are marked with dashed lines.

FIG. 10 : (a) The semi-width of the rivulet a and of the yielded region b, and (b) the maximum thickness of the rivulet h_m and of the yielded region H_m plotted as functions of α/π for $\lambda = 0$, 1/10, 1/4, 1/2 and 1 in the case $\tau_y = 1$ and $\bar{Q} = 1$. For clarity the curves in the special case $\lambda = 0$ are marked with dashed lines.

FIG. 11 : The geometry of the locally unidirectional solution in the yielded zone when $\lambda = 0$.

FIG. 12 : (a) The semi-width of the rivulet a and of the yielded region b, and (b) the maximum thickness of the rivulet h_m and of the yielded region H_m plotted as functions of α/π for $\tau_y = 0$ (in which case the flow is yielded everywhere), 1/5, 1/2, 1, 2 and 5 in the case $\bar{Q} = 1$ and $\lambda = 0$. For clarity the curves in the special case $\tau_y = 0$ (in which $a = b$ and $h_m = H_m$) together with the leading-order asymptotic value in the limit $\tau_y \to \infty$ given by $a \sim \pi/|\cos\alpha|^{1/2}$ for $\pi/2 < \alpha \leq \pi$ are marked with dashed lines.

FIG. 13 : (a) The semi-width of the rivulet a and of the yielded region b, and (b) the maximum thickness of the rivulet h_m and of the yielded region H_m plotted as functions of α/π for $\bar{Q} = 1/5$, 1/2, 1, 2, 5 and 10 in the case $\tau_y = 1$ and $\lambda = 0$. The leading-order asymptotic values in the

limit $\bar{Q} \to 0$ given by $a \sim a_{\mathrm{y}}$ and $h_{\mathrm{m}} \sim \tau_{\mathrm{y}}/\sin\alpha$ for $\alpha_0 < \alpha \leq \pi$, together with the leading-order asymptotic values in the limit $\bar{Q} \to \infty$ given by $a, b \sim \pi/|\cos\alpha|^{1/2}$ for $\pi/2 < \alpha \leq \pi$ and by $h_{\mathrm{m}} \sim 1/(\cos\alpha)^{1/2}$ and $H_{\mathrm{m}} \sim 1/(\cos\alpha)^{1/2} - \tau_{\mathrm{y}}/\sin\alpha$ for $0 \leq \alpha < \pi/2$ are marked with dashed lines. Note that in this case $\alpha_0/\pi = 0.2879$.

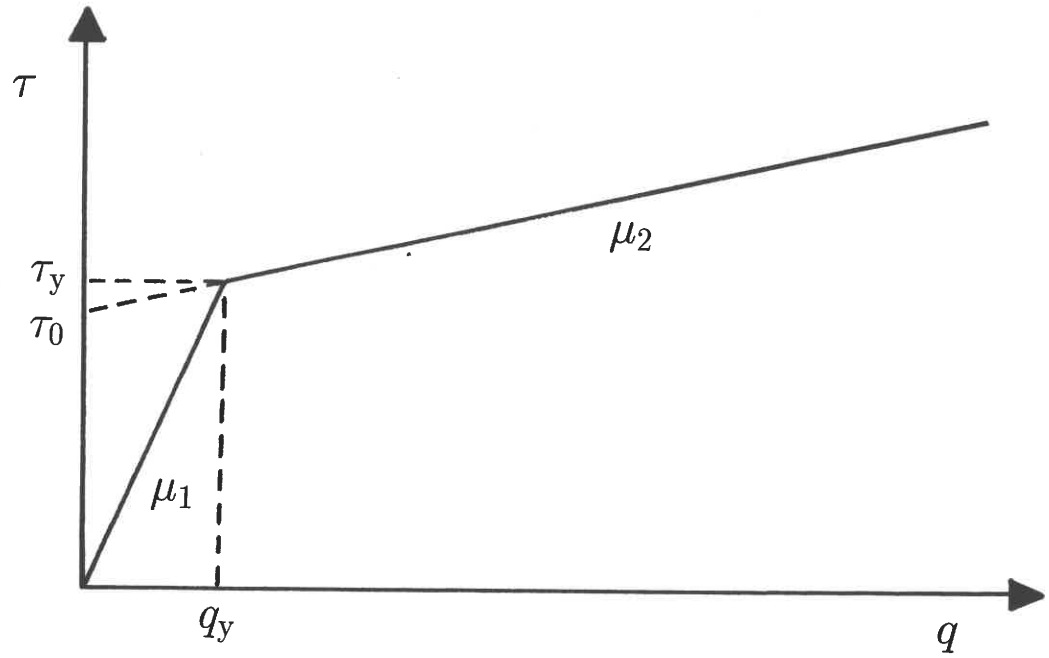

Figure 1 - Wilson, Duffy and Ross

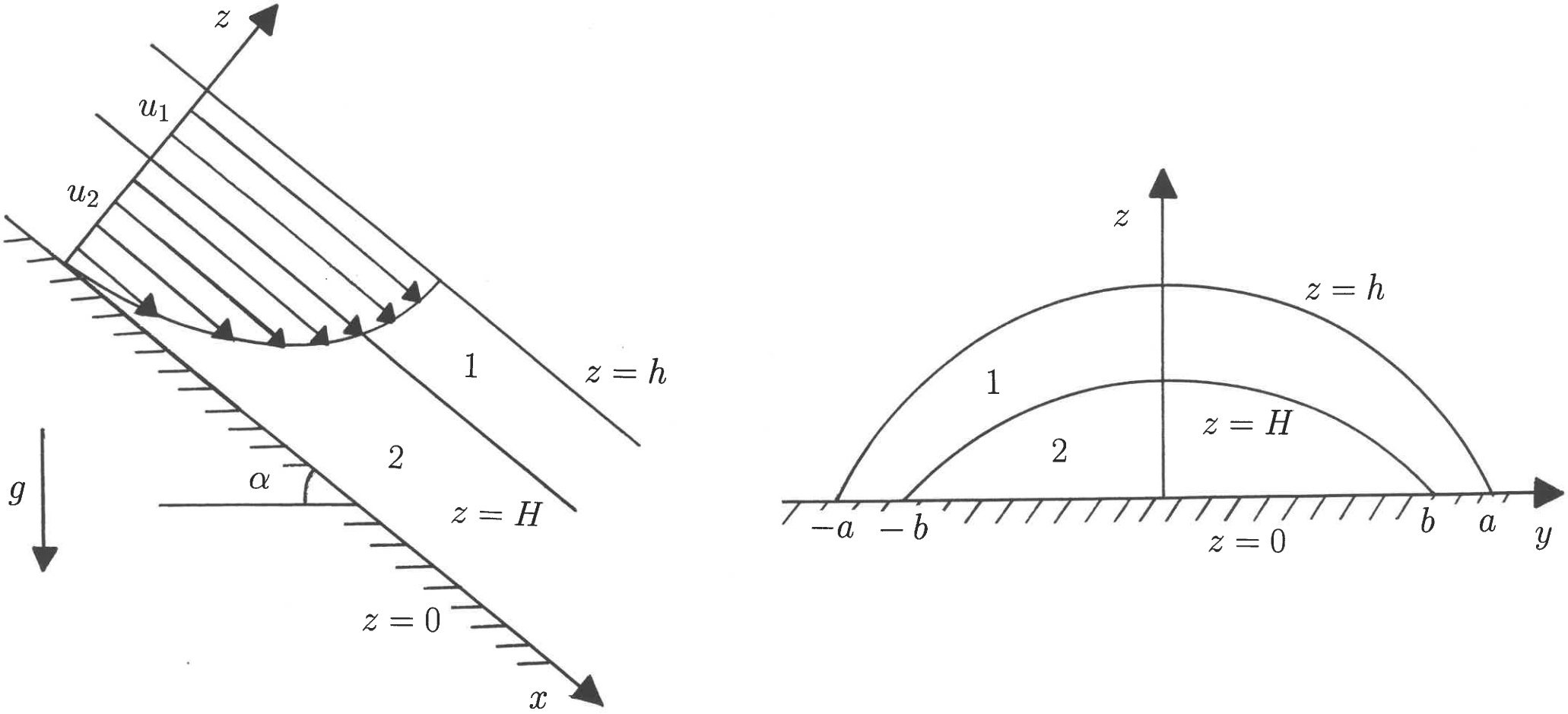

Figure 2 - Wilson, Duffy and Ross

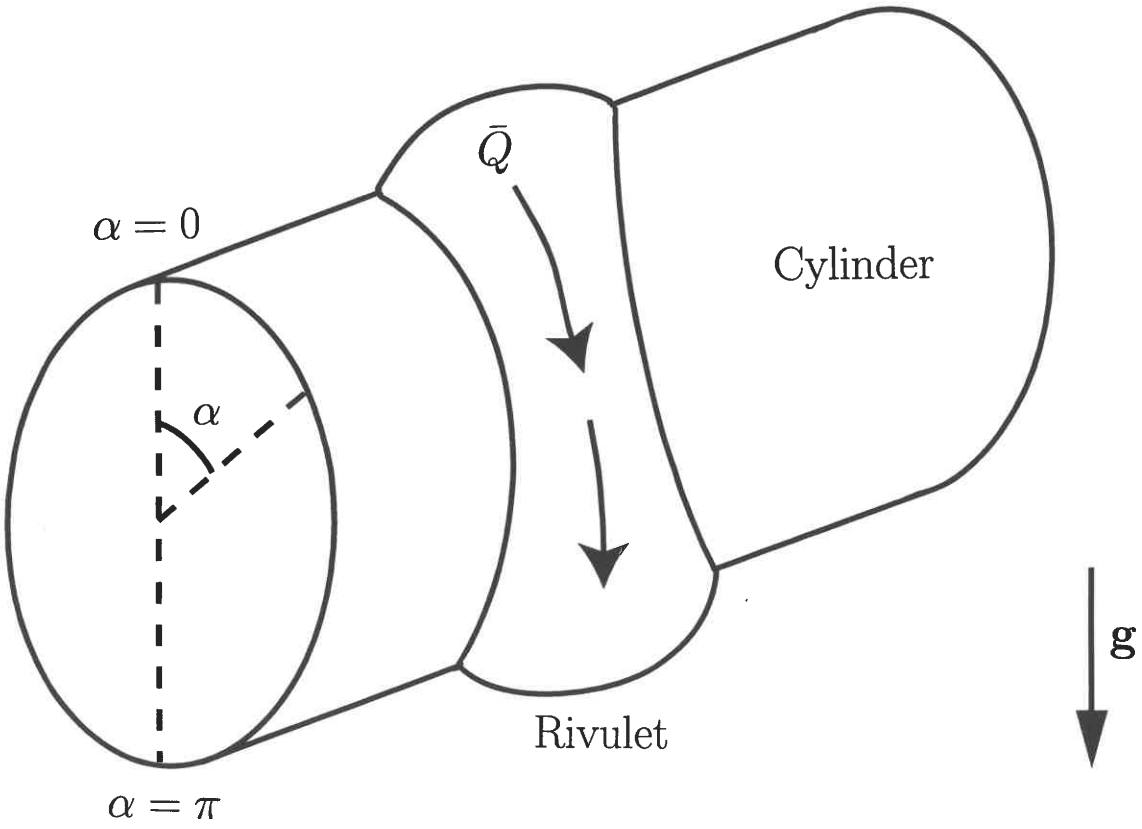

Figure 3 - Wilson, Duffy and Ross

Figure 4 - Wilson, Duffy and Ross

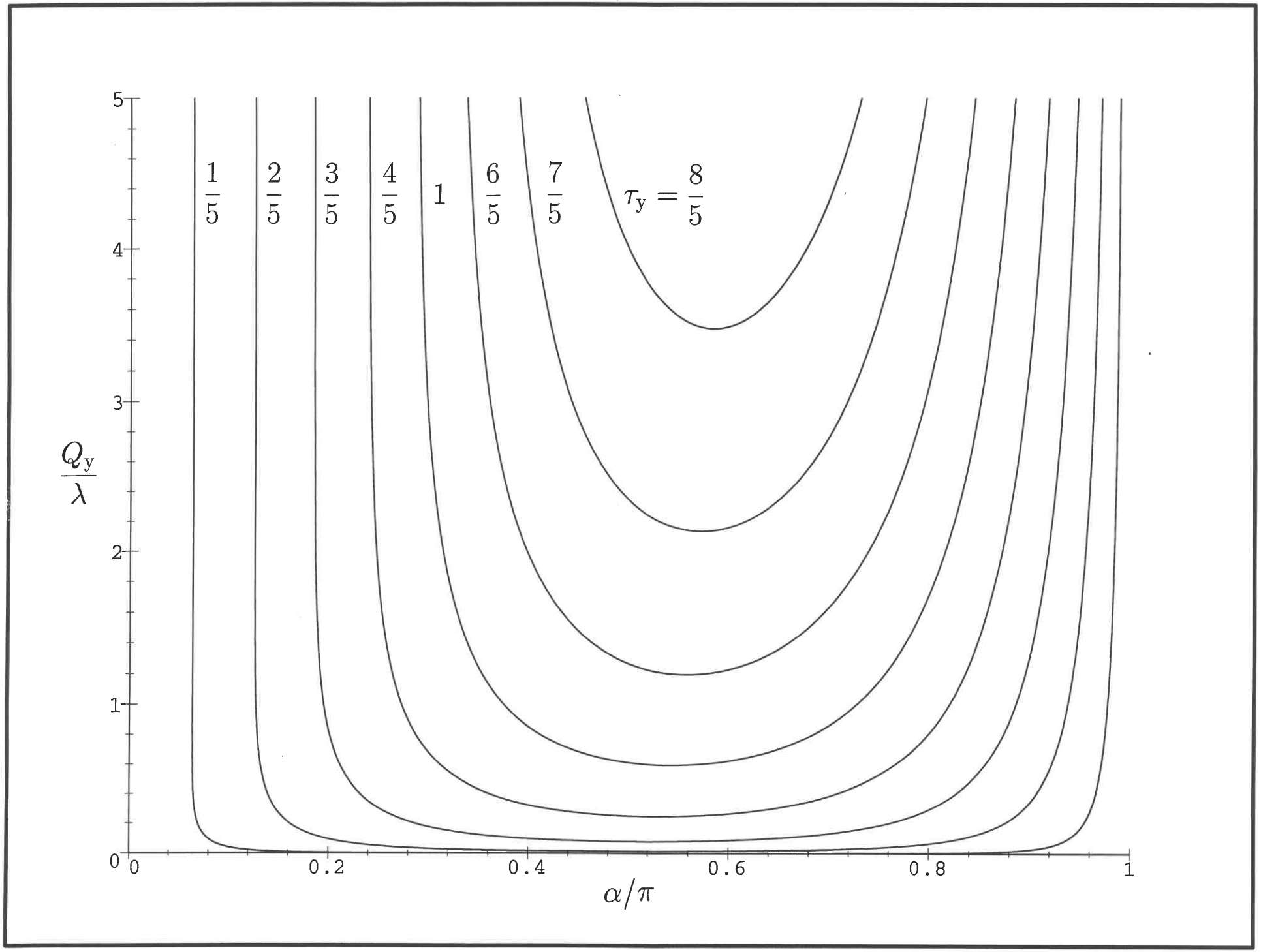

Figure 5(a) - Wilson, Duffy and Ross

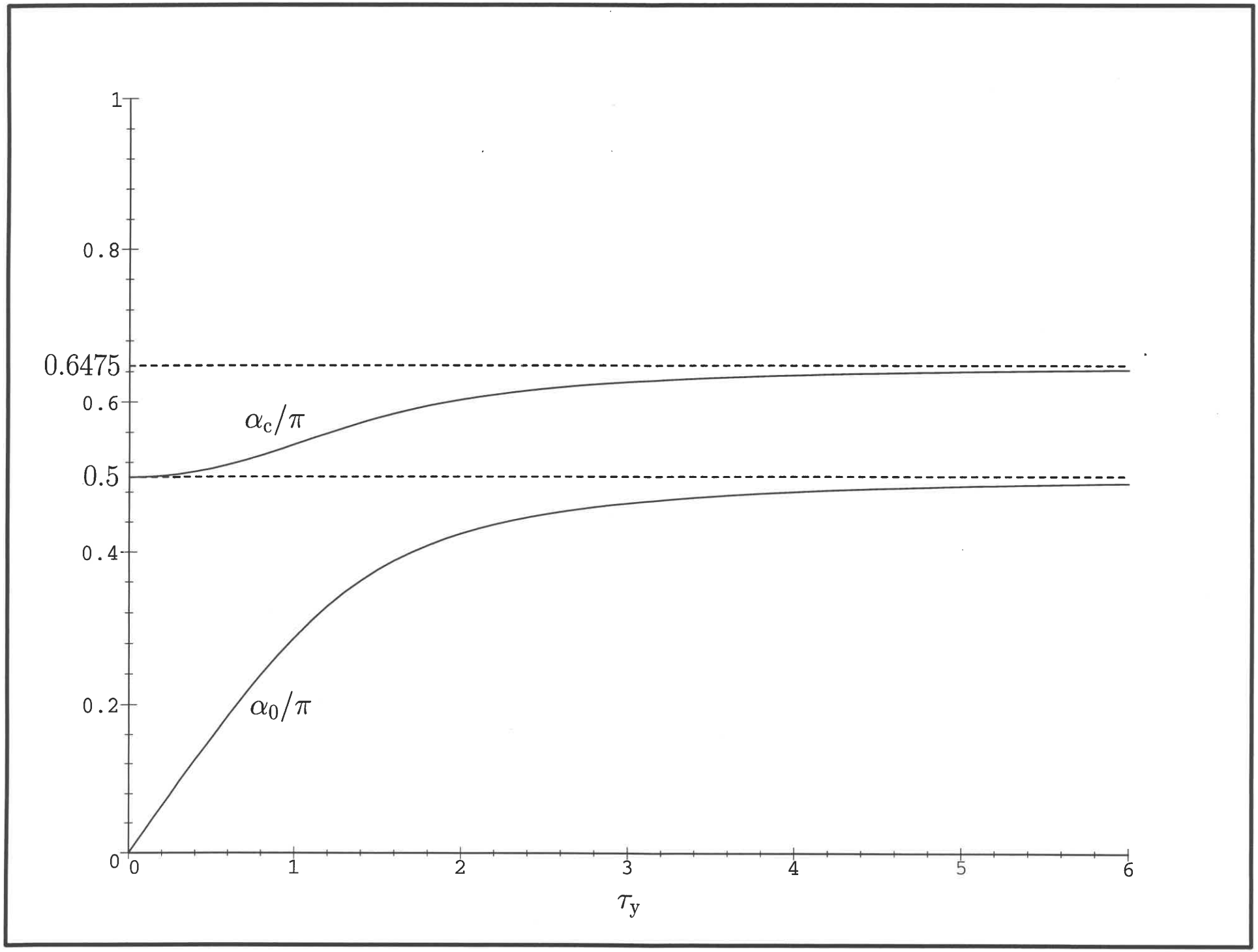

Figure 5(b) - Wilson, Duffy and Ross

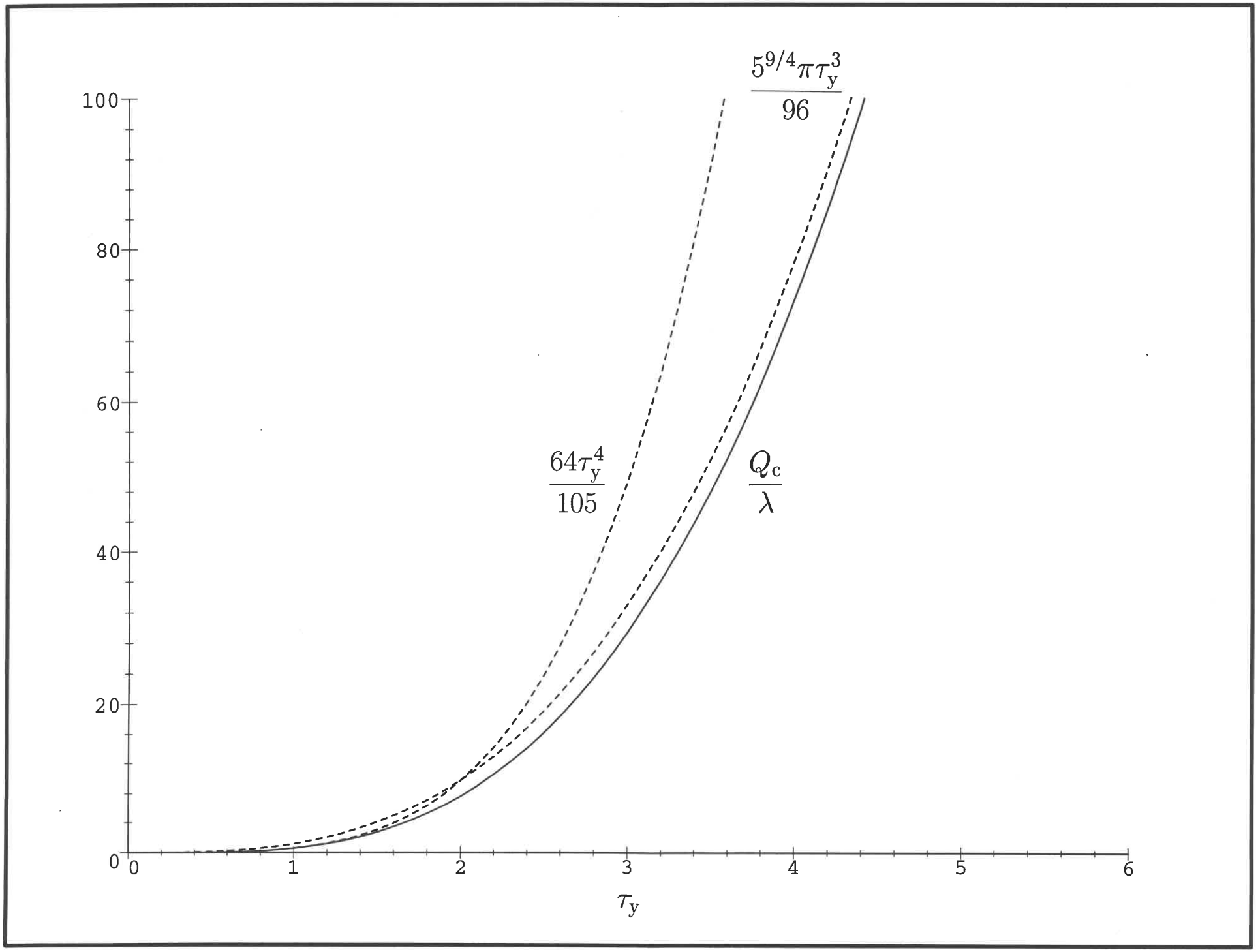

Figure 6(a) - Wilson, Duffy and Ross

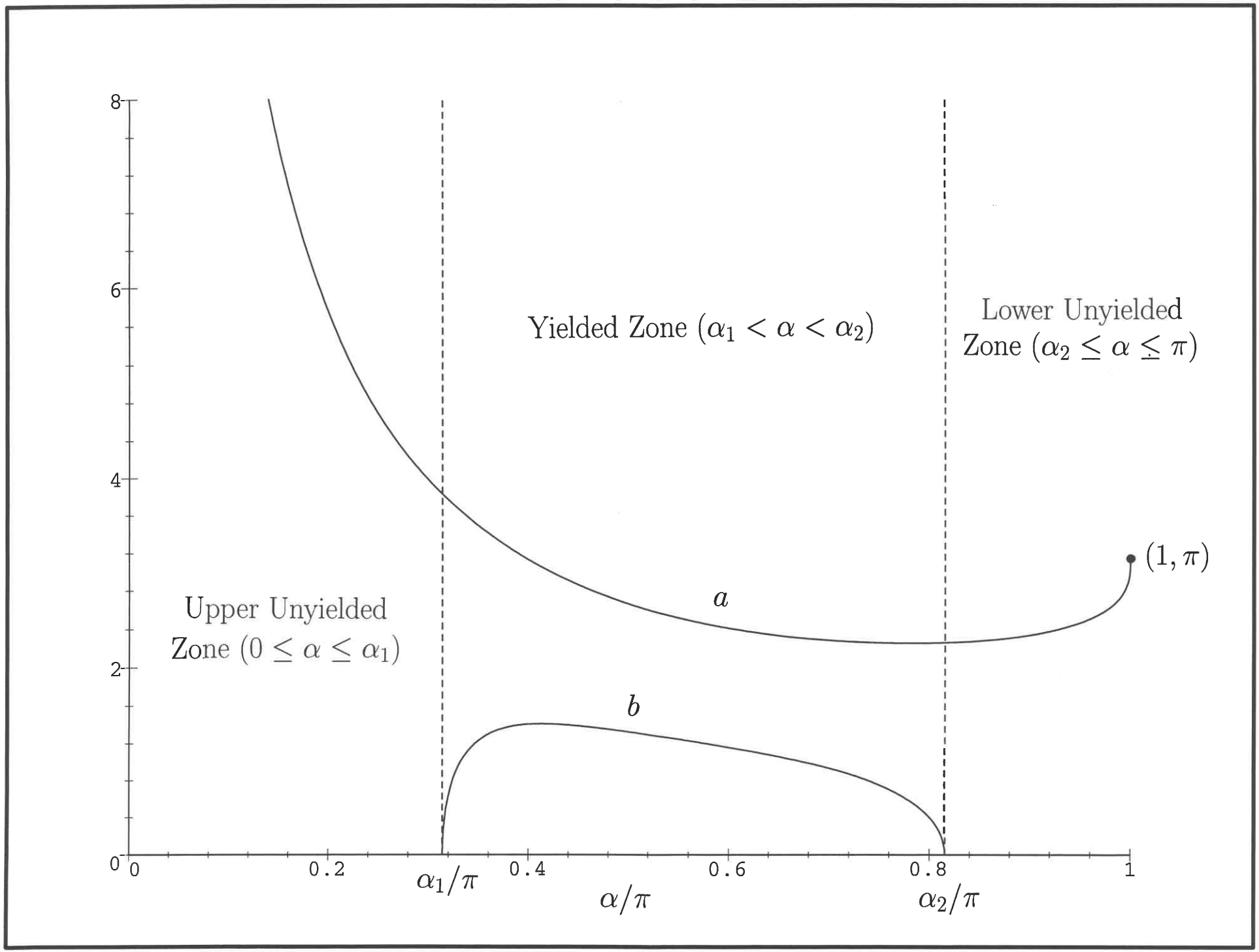

Figure 6(b) - Wilson, Duffy and Ross

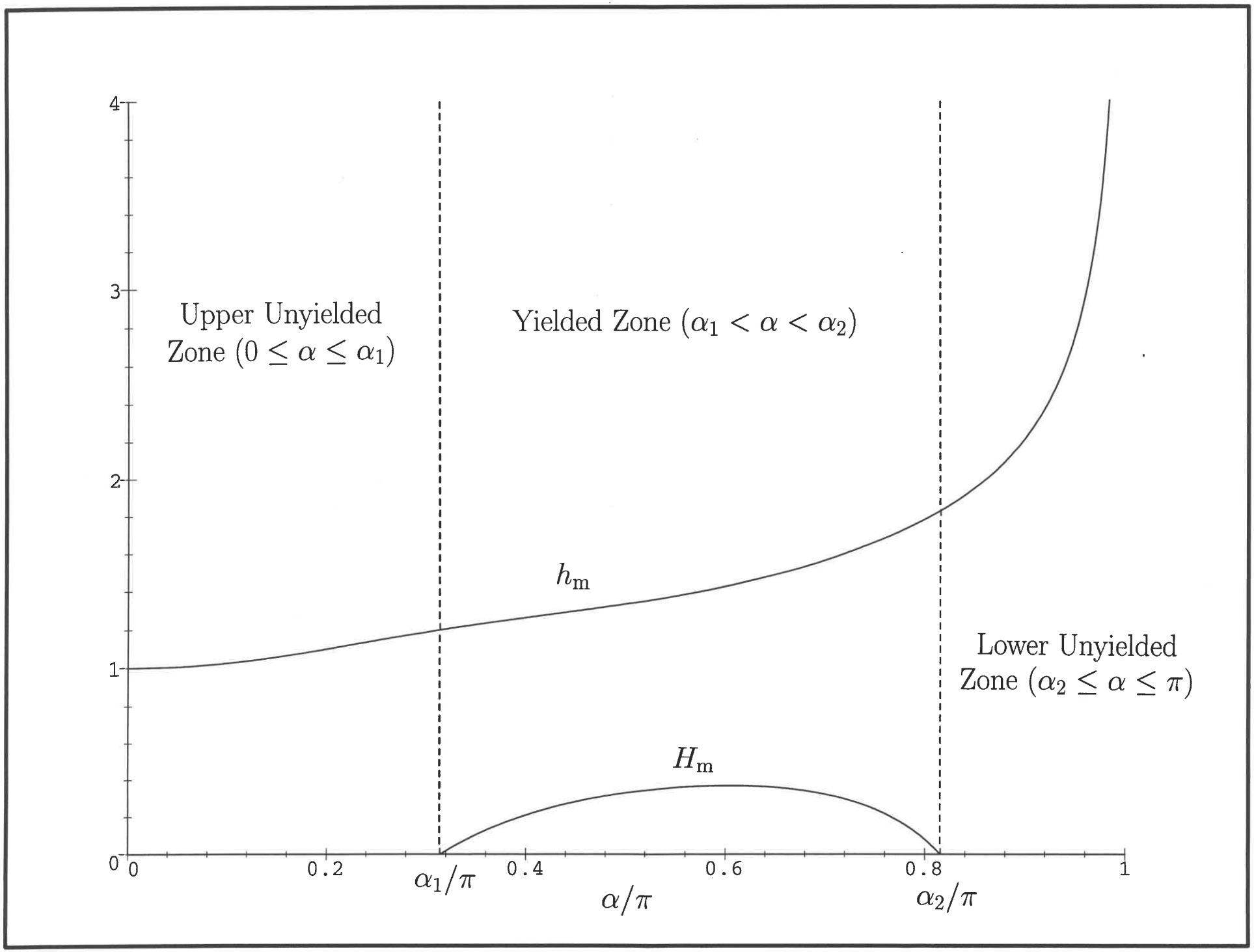

Figure 7(a) - Wilson, Duffy and Ross

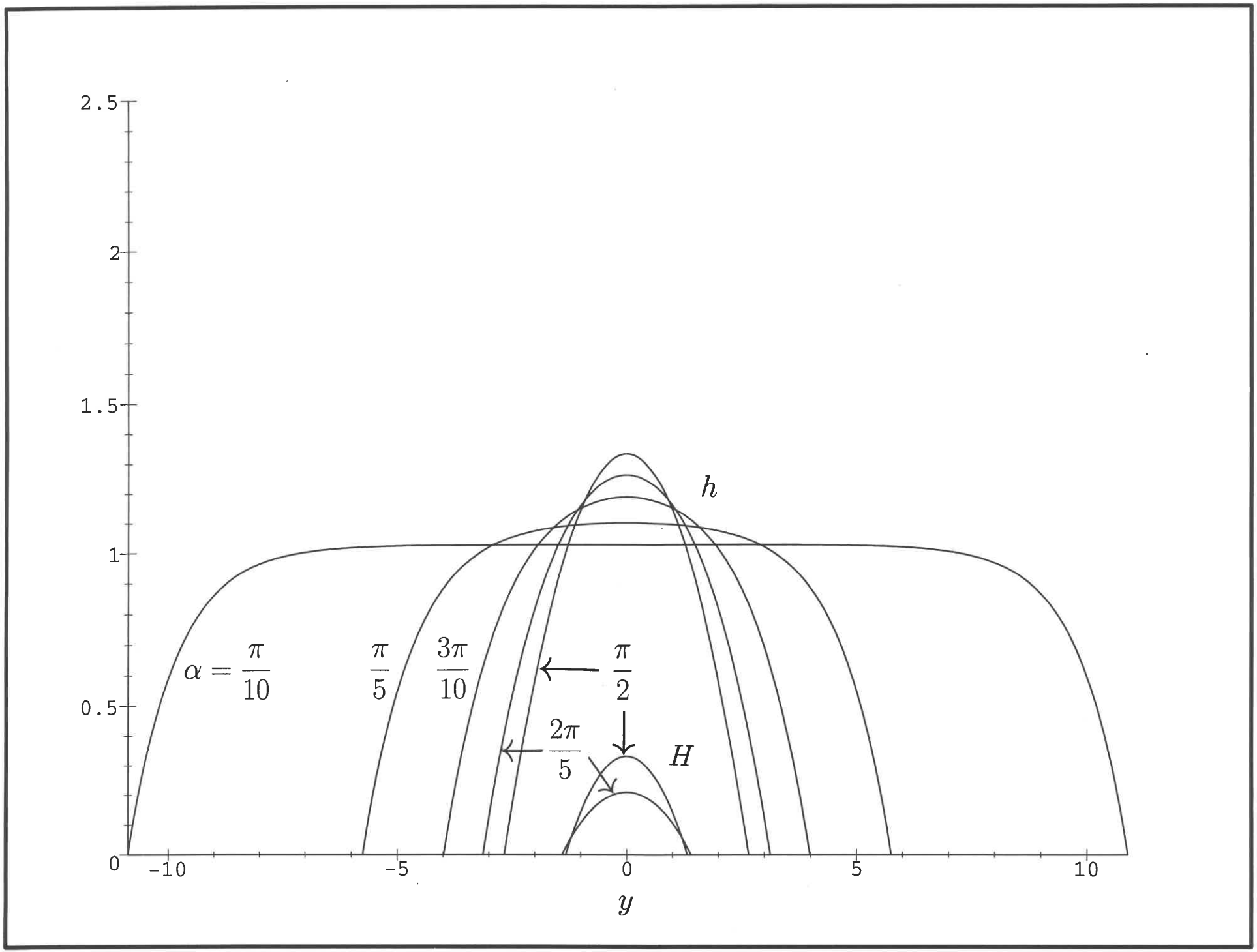

Figure 7(b) - Wilson, Duffy and Ross

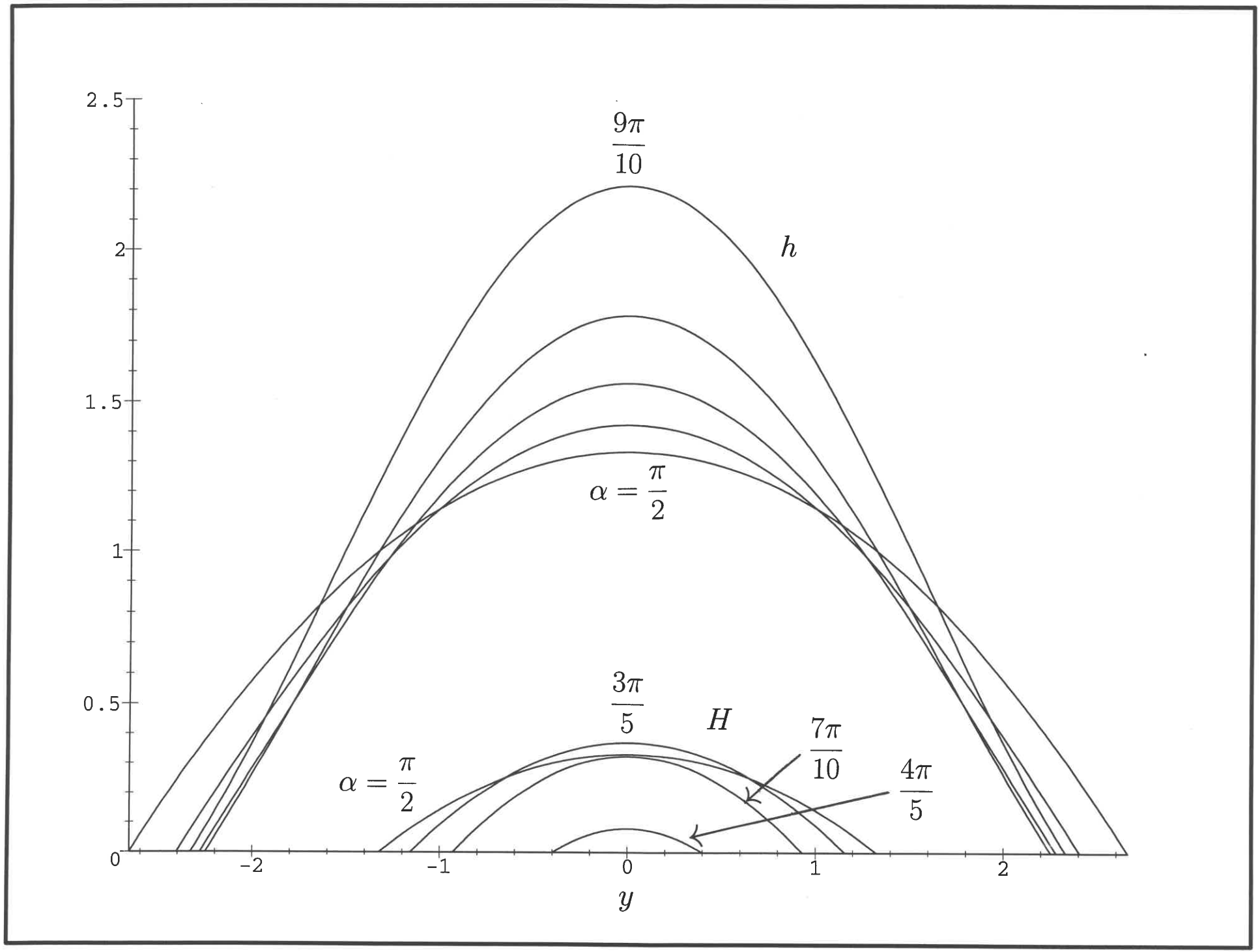

Figure 8(a) - Wilson, Duffy and Ross

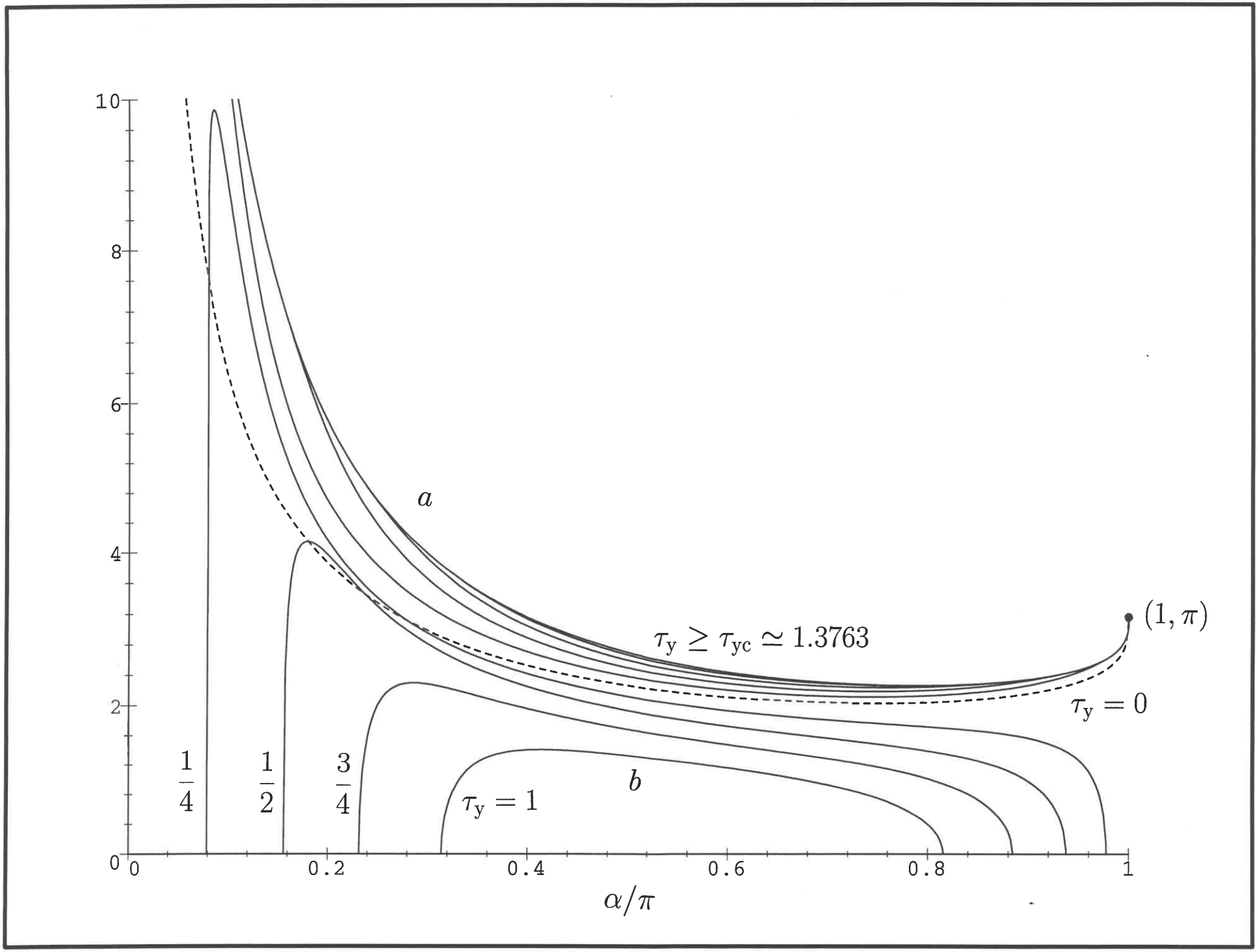

Figure 8(b) - Wilson, Duffy and Ross

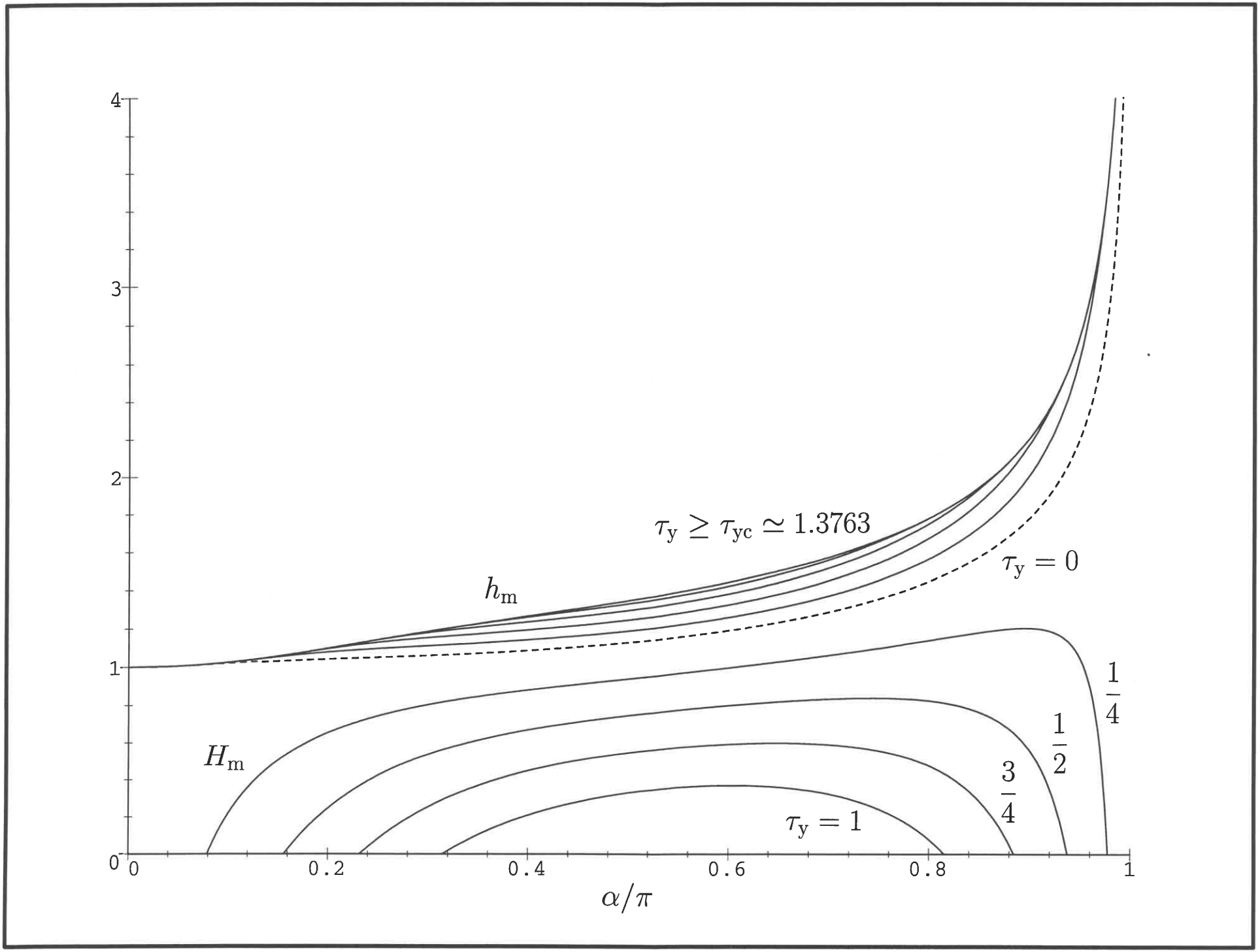

Figure 9(a) - Wilson, Duffy and Ross

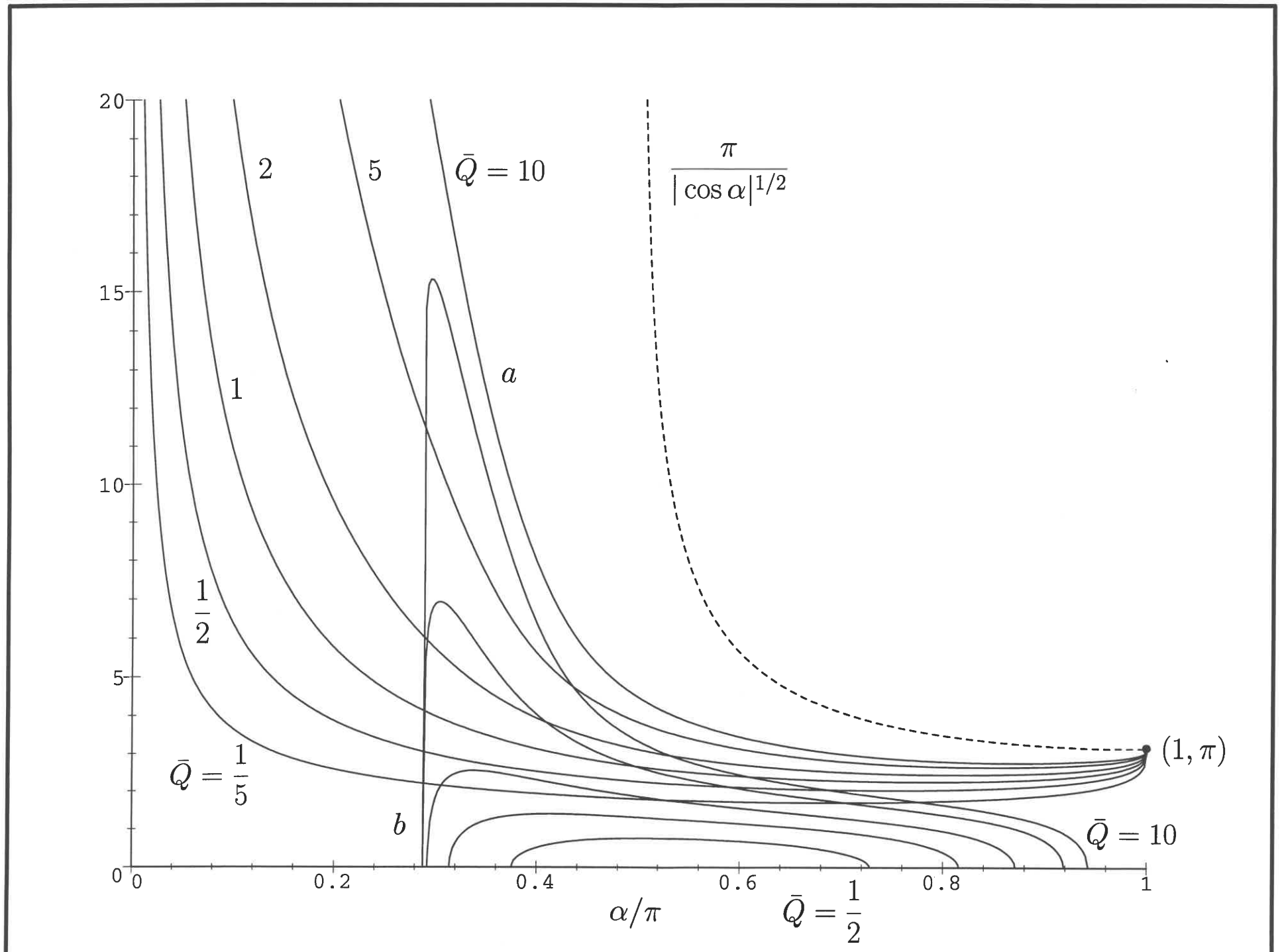

Figure 9(b) - Wilson, Duffy and Ross

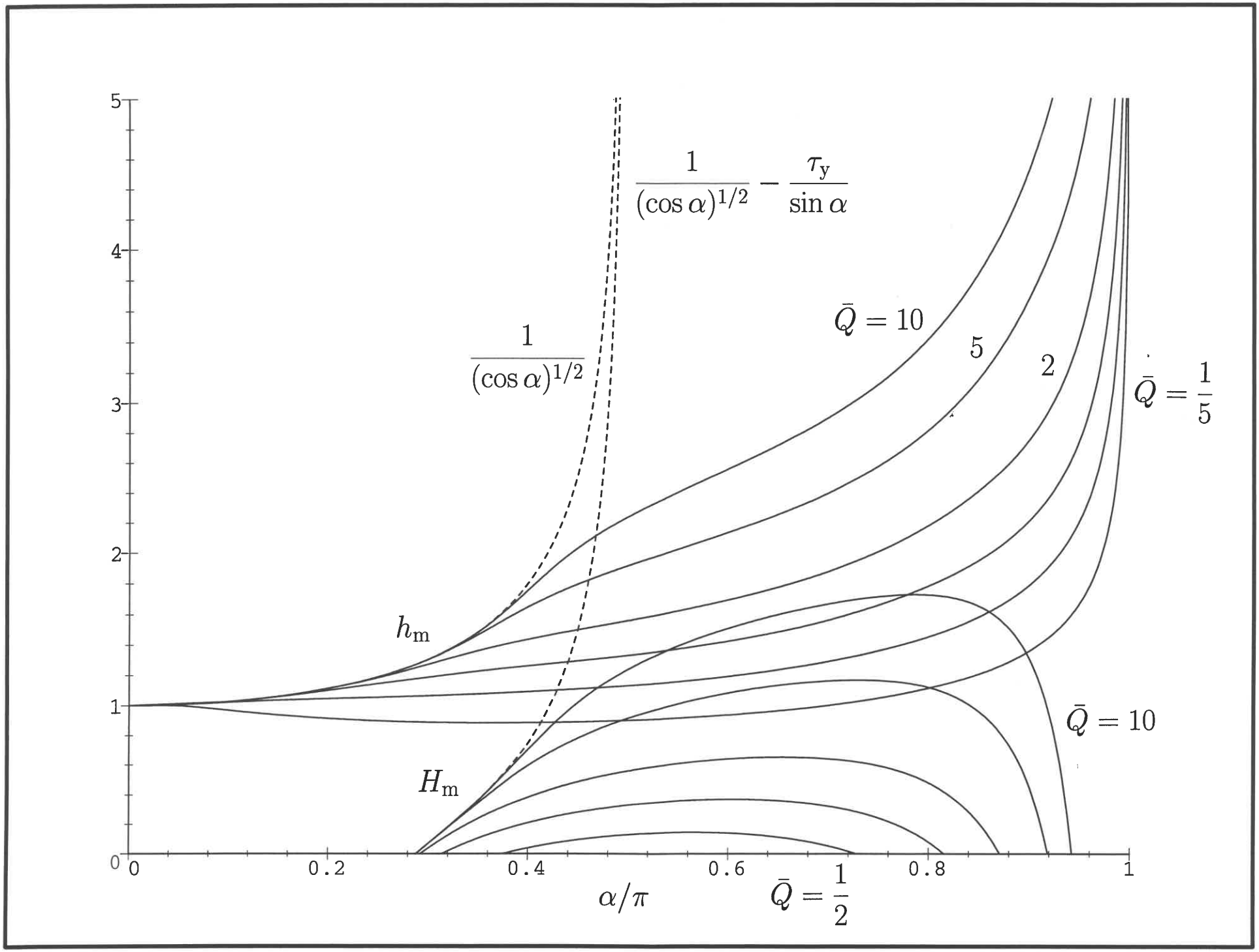

Figure 10(a) - Wilson, Duffy and Ross

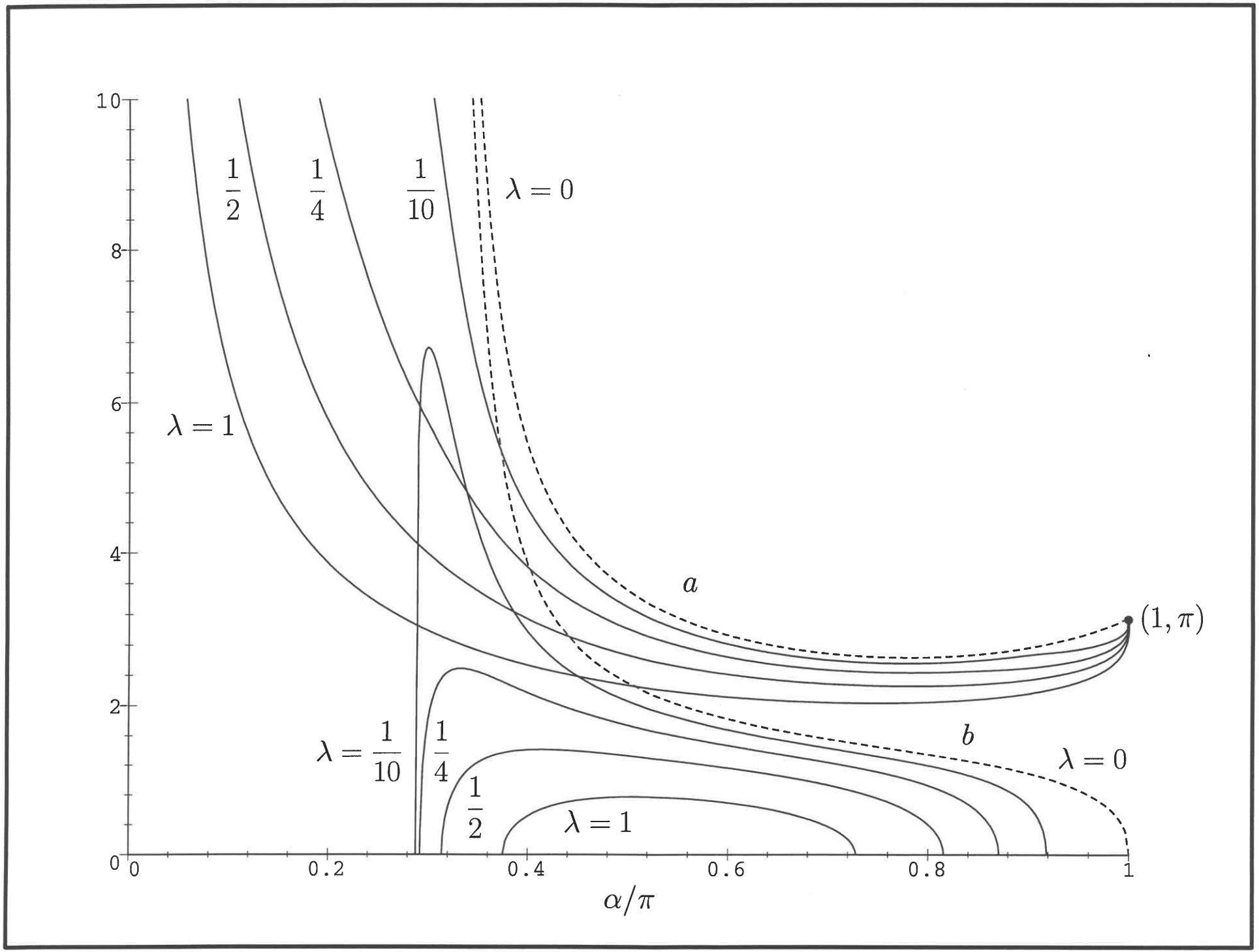

Figure 10(b) - Wilson, Duffy and Ross

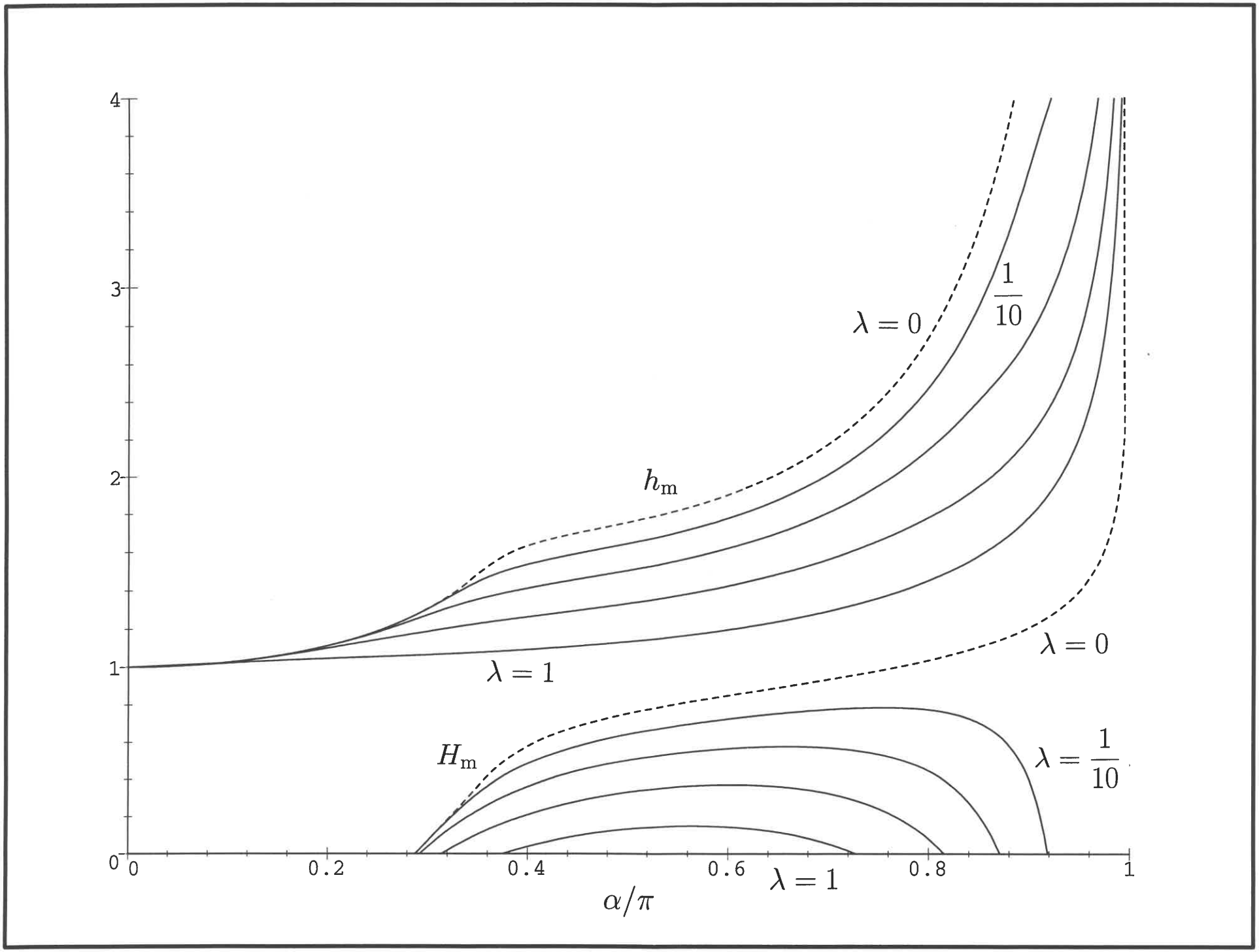

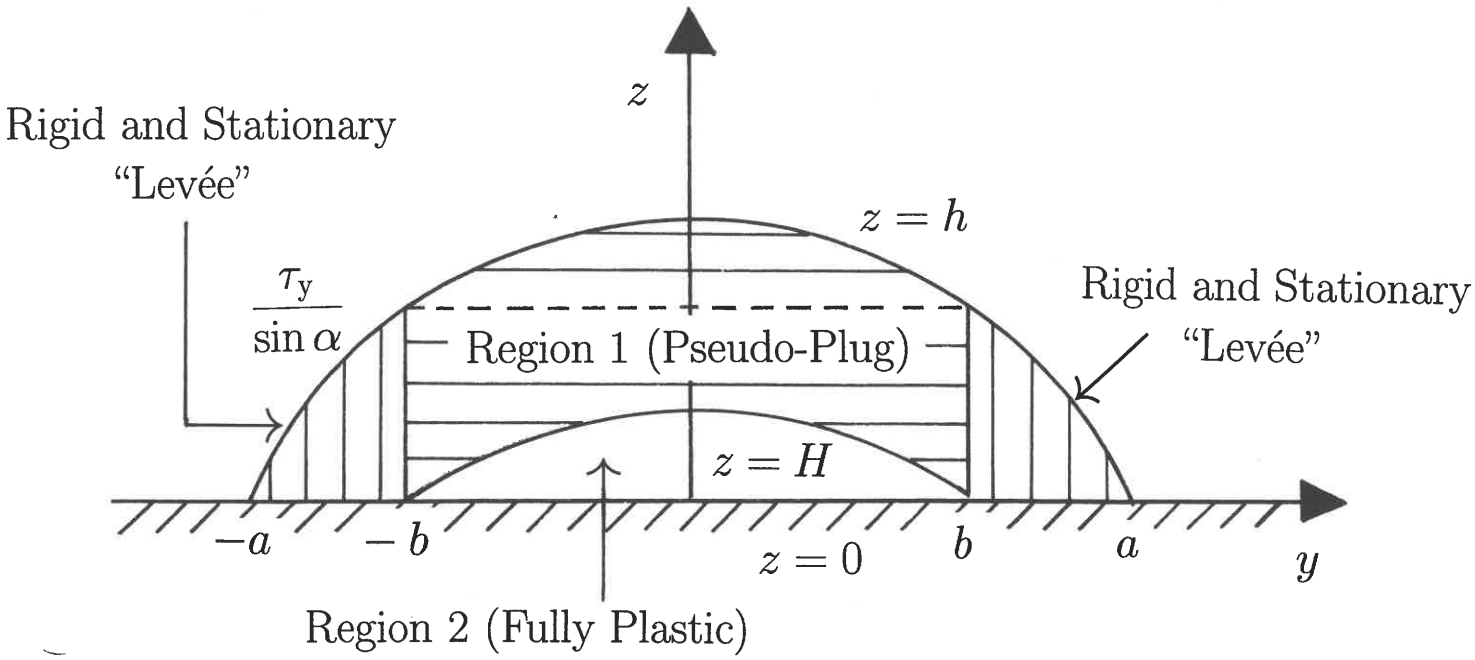

Figure 11 - Wilson, Duffy and Ross

Figure 12(a) - Wilson, Duffy and Ross

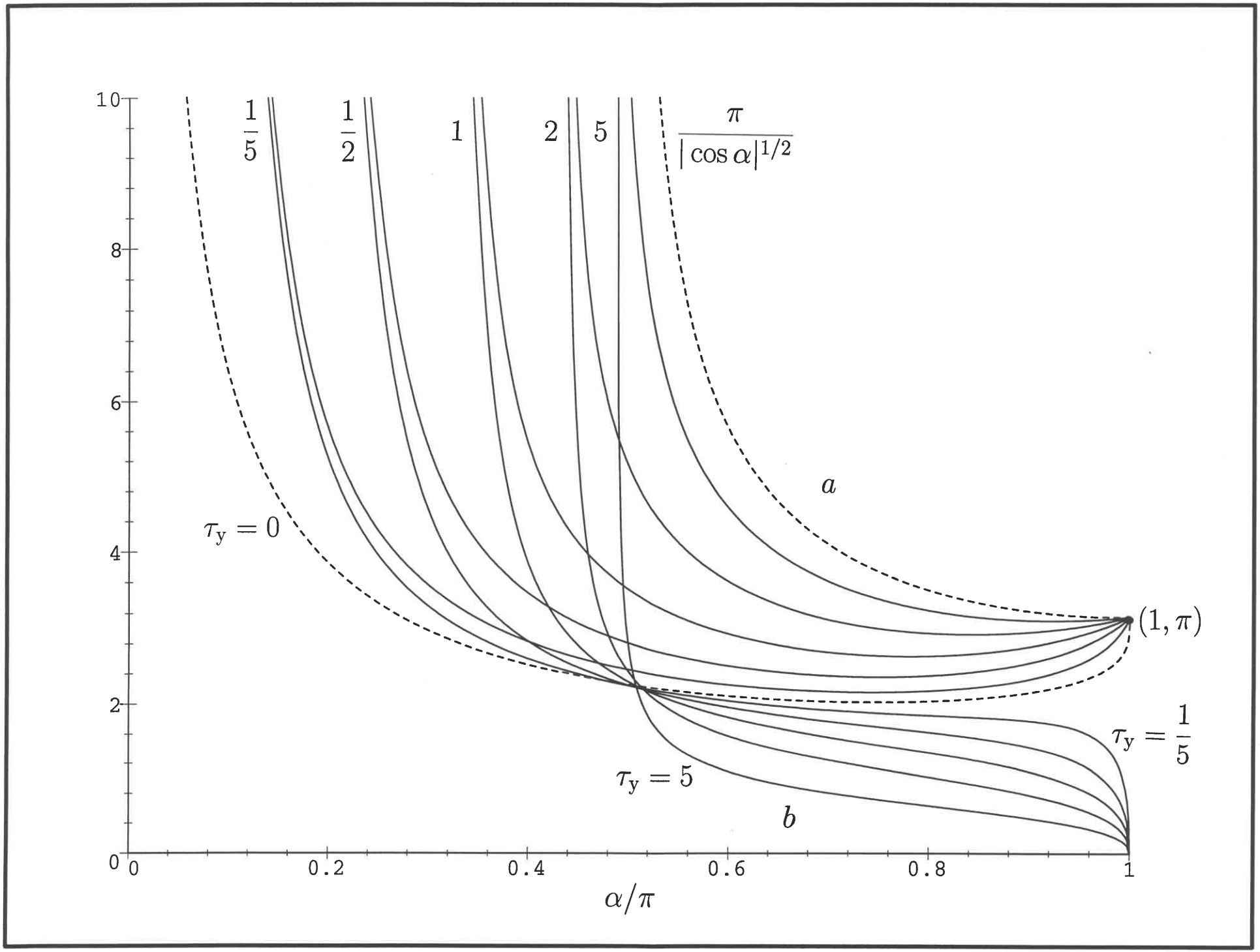

Figure 12(b) - Wilson, Duffy and Ross

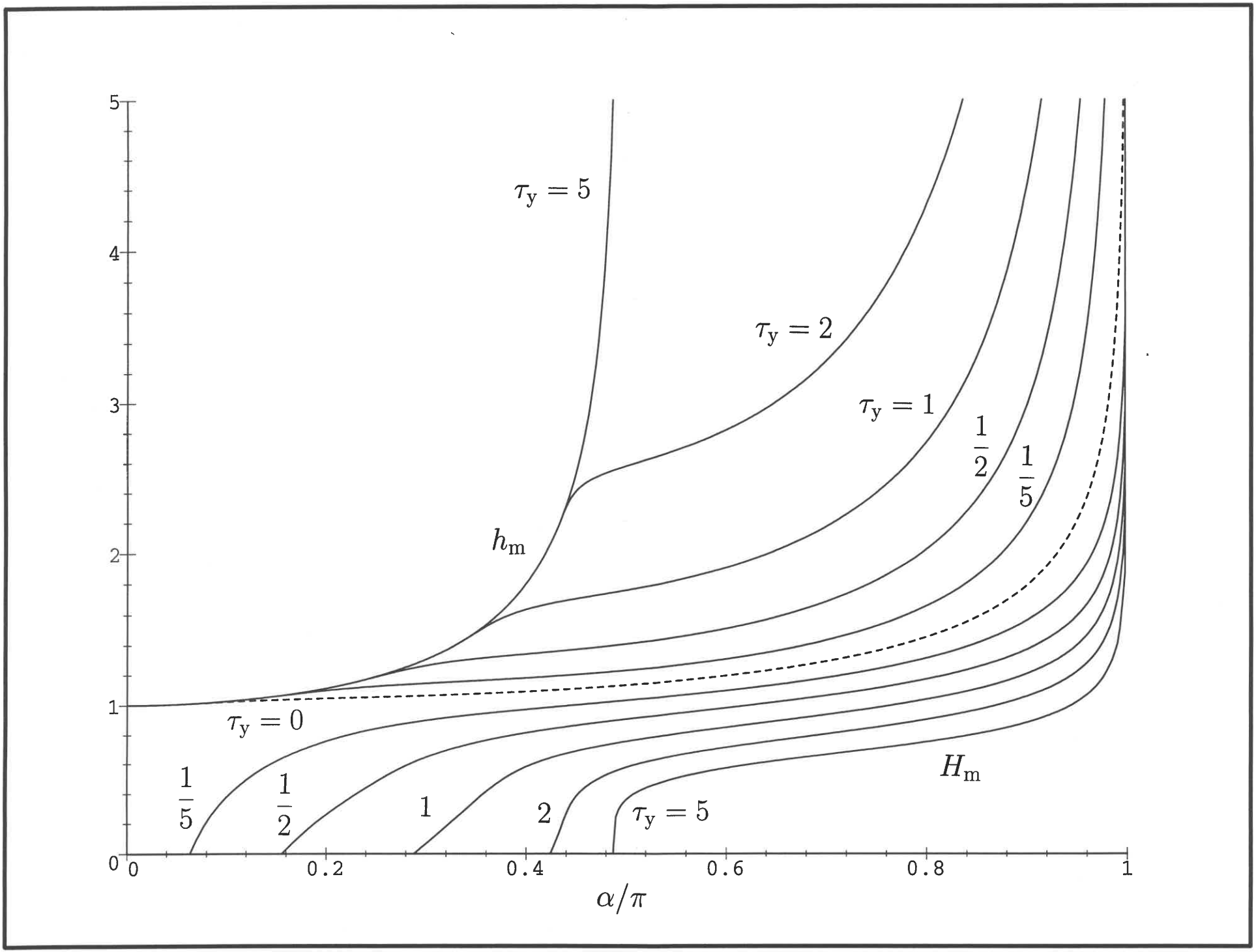

Figure 13(a) - Wilson, Duffy and Ross

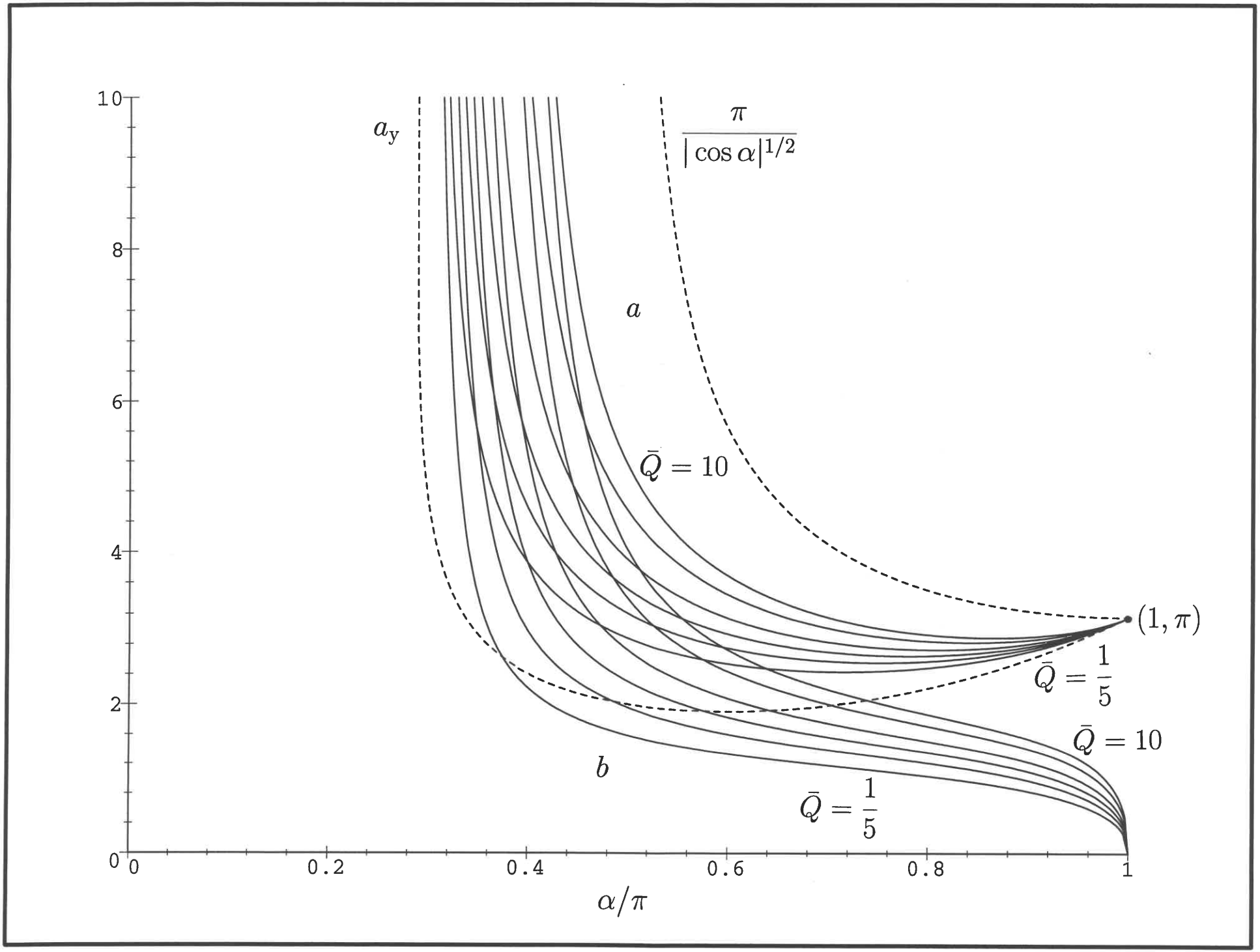

Figure 13(b) - Wilson, Duffy and Ross